

Orbital liquid in ferromagnetic manganites: The orbital Hubbard model for e_g electrons

Louis Felix Feiner

*Institute for Theoretical Physics, Utrecht University, Leuvenlaan 4, NL-3584 CC Utrecht, The Netherlands
and Philips Research Laboratories, Prof. Holstlaan 4, NL-5656 AA Eindhoven, The Netherlands*

Andrzej M. Oleś

*Marian Smoluchowski Institute of Physics, Jagellonian University, Reymonta 4, PL-30059 Kraków, Poland,
and Max-Planck-Institut für Festkörperforschung, Heisenbergstrasse 1, D-70569 Stuttgart, Germany*

(Received 15 July 2004; revised manuscript received 18 January 2005; published 27 April 2005)

We have analyzed the symmetry properties and the ground state of an orbital Hubbard model with two orbital flavors, describing a partly filled spin-polarized e_g band on a cubic lattice, as in ferromagnetic manganites. We demonstrate that the off-diagonal hopping responsible for transitions between x^2-y^2 and $3z^2-r^2$ orbitals, and the absence of $SU(2)$ invariance in orbital space, have important implications. One finds that superexchange contributes in all orbital ordered states, the Nagaoka theorem does not apply, and the kinetic energy is much enhanced as compared with the spin case. Therefore orbital ordered states are harder to stabilize in the Hartree-Fock approximation (HFA), and the onset of a uniform ferro-orbital polarization and antiferro-orbital instability are similar to each other, unlike in the spin case. Next we formulate a cubic (gauge) invariant slave boson approach using the orbitals with complex coefficients. In the mean-field approximation it leads to the renormalization of the kinetic energy and provides a reliable estimate for the ground state energy of the disordered state. Using this approach one finds that the HFA fails qualitatively in the regime of large Coulomb repulsion $U \rightarrow \infty$, where the orbital order is unstable, and instead a strongly correlated *orbital liquid* with disordered orbitals is realized at any electron filling.

DOI: 10.1103/PhysRevB.71.144422

PACS number(s): 75.10.Lp, 75.47.Lx, 71.30.+h, 75.30.Et

I. INTRODUCTION

In recent years there has been renewed interest in orbital degrees of freedom in Mott insulators.¹ Typically, Mott insulators are stoichiometric, i.e., *undoped*, oxides (or sulphides) in which the strong on-site interorbital Coulomb repulsion U on the transition-metal ions dominates over the kinetic energy driven by the electron hopping t and eliminates charge fluctuations. At energies well below U one is then left with effective low-energy interactions $\propto t^2/U$ of superexchange (SE) type. In many cases these are purely magnetic interactions between the spins on the metal ions, leading to the familiar spin models, such as the Heisenberg model. However, when the electrons occupy partly filled degenerate e_g or t_{2g} orbitals, such as in the perovskites KCuF_3 , LaMnO_3 , LaTiO_3 , and LaVO_3 , the orbital degrees of freedom become equally important as the spin ones and it is therefore necessary to treat both of them on equal footing. In such cases the SE is described by so-called spin-orbital models,^{2,3} and the SE interactions are typically strongly frustrated, even on a cubic lattice.⁴ In spin-orbital models the quantum effects are particularly strong—the quantum fluctuations are enhanced, and might even destabilize the long-range magnetic order, leading to a *spin liquid* state, possibly realized in LiNiO_2 .⁴ The opposite situation, that an (isotropic or anisotropic) *orbital liquid* (OL) is stabilized and coexists with long-range spin order, was pointed out recently for t_{2g} Mott-Hubbard systems.⁵ By contrast, in undoped e_g systems, such as KCuF_3 (Ref. 2) and LaMnO_3 (Ref. 6), the quantum phenomena are partly quenched and the SE favors alternating orbital (AO) order which coexists with antiferromagnetic (AF) spin order.

An issue of considerable interest is how such systems, characterized by the presence of orbital degrees of freedom,

behave under doping, and in particular how this compares with the more familiar behavior of doped spin systems. In this paper we address this issue by studying a generic model of correlated e_g electrons with two orbital flavors, described by a pseudospin $T=1/2$ in the orbital Hilbert space, and consider its relation to the standard (spin) Hubbard model for electrons with spin $S=1/2$. So we introduce the *e_g -orbital Hubbard model* and investigate: (i) in what respect long-range order in such an *orbital system* is different from that in the analogous *spin system*, and (ii) whether the orbitals may order when U is large, or rather form a *disordered* OL. These questions are of fundamental nature and our main aim in addressing them is to uncover and elucidate the *physical mechanisms* which operate in the e_g band and are typical for orbital degeneracy, in particular by contrasting them with those known to operate in spin systems.

The present problem is closely related to the physical properties of the colossal magnetoresistance (CMR) manganites,⁷ where the well-known mechanism of double exchange introduced by Zener⁸ is responsible for the metallic ferromagnetic (FM) phase at finite doping, in which the spins of the e_g electrons are fully polarized. The model that we will investigate here covers only the case of the FM phase, thus neglecting the competition of the double-exchange mechanism with the spin AF SE, and the resulting dependence of the hopping amplitude on the actual spin states at two neighboring sites.⁹ Even when one limits oneself to the FM phase, a sequence of orbital-ordered phases may be expected,¹⁰ and each of them would break cubic symmetry, contrary to what is observed in the magnetic properties of the metallic FM phase. The analysis of the present paper, making extensive use of the auxiliary particle method in the strongly correlated

regime,¹¹ provides the basis for a proper treatment of this problem,¹² which enables one to understand the persistence of cubic symmetry and more in particular why the magnon stiffness constant increases with hole doping.¹³

This paper is organized as follows. In Sec. II we introduce the orbital Hubbard model for spin-polarized e_g electrons at orbital degeneracy and discuss its symmetry properties. We show that the cubic symmetry of the hopping may be better appreciated when a particular basis consisting of two orbitals with complex coefficients is used. Next we analyze in Sec. III the possible orbital ordered phases at $U=\infty$ and compare their densities of states and total energies derived within the slave fermion formalism. Such phases follow from the instabilities towards orbital-ordered states obtained within the Hartree-Fock (HF) approximation (Sec. IV), and we show that such instabilities and the properties of the ordered phases at finite U , related to the SE, are here quite different from those known from the spin Hubbard model. In Sec. V we introduce the cubic invariant slave boson approach and use the mean-field approximation to analyze the disordered orbital liquid state. Within a generalization of the Kotliar-Ruckenstein¹⁴ (KR) approach to the present orbital problem, we give reasons why the orbital ordered states are unstable against the OL disordered state when one goes beyond the HF approximation. The paper is concluded in Sec. VI by pointing out the implications of our results for the physical properties of the CMR manganites.

II. ORBITAL HUBBARD MODEL

A. The Hamiltonian and its symmetry properties

We consider spinless e_g electrons on a cubic lattice with kinetic energy

$$H_t = -t \sum_{\alpha} \sum_{\langle ij \rangle \alpha} c_{i\alpha}^{\dagger} c_{j\alpha}, \quad (2.1)$$

where hopping with amplitude $-t$ between sites i and j occurs only for a pair of directional orbitals $|\zeta_{\alpha}\rangle$ oriented along the bond $\langle ij \rangle$ direction, i.e., $|\zeta_{\alpha}\rangle \propto 3x^2 - r^2$, $3y^2 - r^2$, and $3z^2 - r^2$, when the bond $\langle ij \rangle$ is along the cubic axis $\alpha = a, b$, and c , respectively. We will similarly denote by $|\xi_{\alpha}\rangle$ the orbital which is orthogonal to $|\zeta_{\alpha}\rangle$ and is oriented perpendicular to the bond $\langle ij \rangle$, i.e., $|\xi_{\alpha}\rangle \propto y^2 - z^2$, $z^2 - x^2$, and $x^2 - y^2$, for a bond $\langle ij \rangle$ along the axis $\alpha = a, b$, and c , respectively. While such a choice of basis, that depends on the bond direction under consideration, is convenient for writing down the kinetic energy, one cannot avoid to choose a particular orthogonal basis for the two orbital flavors as soon as one wants to introduce a Hubbard term to describe the local electron interactions. The usual choice is to take

$$|z\rangle \equiv \frac{1}{\sqrt{6}}(3z^2 - r^2), \quad |x\rangle \equiv \frac{1}{\sqrt{2}}(x^2 - y^2), \quad (2.2)$$

called *real orbitals*. However, because this basis is the natural one only for the bonds parallel to the c axis but not for those in the (a, b) plane, the kinetic energy then takes the form^{15,16}

$$H_t = -\frac{1}{4}t \sum_{\langle ij \rangle \parallel a, b} [3c_{ix}^{\dagger}c_{jx} + c_{iz}^{\dagger}c_{jz} \mp \sqrt{3}(c_{ix}^{\dagger}c_{jz} + c_{iz}^{\dagger}c_{jx})] - t \sum_{\langle ij \rangle \parallel c} c_{iz}^{\dagger}c_{jz}, \quad (2.3)$$

and although this expression is of course cubic invariant, the representation (2.3) of the hopping does not exhibit this symmetry but takes a very different appearance depending on the bond direction.

We thus prefer to use instead the basis of *complex orbitals* at each site¹⁷

$$|+\rangle = \frac{1}{\sqrt{2}}(|z\rangle - i|x\rangle), \quad |-\rangle = \frac{1}{\sqrt{2}}(|z\rangle + i|x\rangle), \quad (2.4)$$

corresponding to “up” and “down” pseudospin flavors, with the local pseudospin operators defined as

$$T_i^{\pm} = c_{i\pm}^{\dagger}c_{i\pm}, \quad T_i^{-} = c_{i\pm}^{\dagger}c_{i\mp},$$

$$T_i^z = \frac{1}{2}(c_{i+}^{\dagger}c_{i+} - c_{i-}^{\dagger}c_{i-}) = \frac{1}{2}(n_{i+} - n_{i-}). \quad (2.5)$$

For later reference it is convenient to introduce also electron creation operators $c_i^{\dagger}(\psi_i, \theta_i)$ which create e_g electrons in orbital coherent states, defined as

$$|\Omega_i\rangle = e^{-i\theta_i/2} \cos\left(\frac{\psi_i}{2}\right)|i+\rangle + e^{+i\theta_i/2} \sin\left(\frac{\psi_i}{2}\right)|i-\rangle, \quad (2.6)$$

in analogy with the well-known spin coherent states.¹⁸ The expectation value of the local pseudospin operator in the coherent orbital (2.6) behaves like a classical vector,¹⁹

$$\langle \Omega_i | T_i | \Omega_i \rangle = \frac{1}{2}(\sin \psi_i \cos \theta_i, \sin \psi_i \sin \theta_i, \cos \psi_i), \quad (2.7)$$

traversing a sphere, with the “equatorial plane” ($\psi_i = \pi/2$) corresponding to real orbitals $|\Omega_i(\pi/2, \theta_i)\rangle \equiv |i\theta_i\rangle = \cos(\theta_i/2)|iz\rangle - \sin(\theta_i/2)|ix\rangle$, and the “poles” ($\psi_i = 0$ and $\psi_i = \pi$) to the complex orbitals $|i+\rangle$ and $|i-\rangle$. The three directional orbitals $|i\zeta_{\alpha}\rangle$ at site i , associated with the three cubic axes ($\alpha = a, b, c$) are the real orbitals with θ_i being equal to $\vartheta_a = -4\pi/3$, $\vartheta_b = +4\pi/3$, and $\vartheta_c = 0$, respectively, i.e.,

$$|i\zeta_{\alpha}\rangle = \frac{1}{\sqrt{2}}[e^{-i\vartheta_{\alpha}/2}|i+\rangle + e^{+i\vartheta_{\alpha}/2}|i-\rangle] = \cos(\vartheta_{\alpha}/2)|iz\rangle - \sin(\vartheta_{\alpha}/2)|ix\rangle, \quad (2.8)$$

and thus correspond to the pseudospin lying in the equatorial plane and pointing in one of the three equilateral “cubic” directions defined by the angles ϑ_{α} .

In the complex-orbital representation (2.4) the *orbital Hubbard model* for e_g electrons takes the form

$$\mathcal{H} = -\frac{1}{2}t \sum_{\alpha} \sum_{\langle ij \rangle \parallel \alpha} [(c_{i+}^{\dagger}c_{j+} + c_{i-}^{\dagger}c_{j-}) + \gamma(e^{-i\chi_{\alpha}}c_{i+}^{\dagger}c_{j-} + e^{+i\chi_{\alpha}}c_{i-}^{\dagger}c_{j+})] + U \sum_i n_{i+}n_{i-}, \quad (2.9)$$

with $\chi_a = +2\pi/3$, $\chi_b = -2\pi/3$, and $\chi_c = 0$, and where the

newly introduced parameter γ , explained below, takes the value $\gamma=1$. The appearance of the phase factors $e^{\pm i\chi_\alpha}$ is characteristic of the orbital problem—they occur because the orbitals have an actual shape in real space so that each hopping process depends on the bond direction. The form of the interorbital Coulomb interaction $\propto U$ is invariant under any local basis transformation to a pair of orthogonal orbitals; it gives an energy U either when two real orbitals are simultaneously occupied, $U\sum_i n_{i_x}n_{i_z}$, or when two complex orbitals are occupied, as in Eq. (2.9).

The representation (2.9) has several advantages: (i) It displays manifestly the cubic symmetry, since the transformation $\chi_\alpha \rightarrow \chi_\alpha - 2\pi/3$ [which amounts in Eq. (2.9) to the cyclic permutation $a \rightarrow b \rightarrow c \rightarrow a$ of the cubic axes] in conjunction with the corresponding phase shift of the electron operators $c_{i\pm}^\dagger \rightarrow c_{i\pm}^\dagger e^{\pm 2i\pi/3}$ (which permutes the $|\zeta_\alpha\rangle$ -orbitals according to $3x^2 - r^2 \rightarrow 3y^2 - r^2 \rightarrow 3z^2 - r^2 \rightarrow 3x^2 - r^2$) leaves the Hamiltonian (2.9) invariant. (ii) It exhibits clearly the difference between the spin case and the orbital case. In the orbital case there is both pseudospin-conserving hopping [the first line in Eq. (2.9)] and *pseudospin-nonconserving hopping* [the second line in Eq. (2.9)], whereas in the corresponding spin case, i.e., in the standard Hubbard model, there is of course only spin-conserving hopping and the second term is absent. Thus the present complex-orbital representation allows us to introduce the parameter γ by which one can turn the e_g -band orbital Hubbard model ($\gamma=1$) into what is formally a spin Hubbard model with the same hopping amplitudes ($\gamma=0$), interpreting “+” and “−” as “spin up” and “spin down.” This device makes it very easy to recognize the differences in physical behavior between the orbital case and the spin case: the parameter γ will of course show up in all analytical expressions below, and one can compare at a glance the result for the orbital case ($\gamma=1$) with that for the spin case ($\gamma=0$). At the present stage one can already observe from Eq. (2.9) that there is *more* kinetic energy available per electron in the orbital case, because additional hopping channels are present. We will see below that this has important consequences for the relative stability of various states. (iii) Finally, it shows explicitly that rotational $SU(2)$ symmetry for the pseudospins is absent,² which in the complex-orbital representation is immediately obvious from the presence of the pseudospin-nonconserving hopping term $\propto \gamma$ in Eq. (2.9). Thus the components of the total pseudospin operator $\mathcal{T} = \sum_i \mathcal{T}_i$ are conserved only at $\gamma=0$ (i.e., $[\mathcal{T}, \mathcal{H}] = 0$), while the terms $\propto \gamma$ in \mathcal{H} commute instead with the staggered pseudospin operator $\mathcal{T}_Q^z = \sum_i \exp(i\mathbf{Q} \cdot \mathbf{R}_i) T_i^z$, where $\mathbf{Q} = (\pi, \pi, \pi)$.

B. New features compared with the spin case

It is instructive to follow the changes of the electronic structure of the uncorrelated band [i.e., with $U=0$ in Eq. (2.9)] with increasing γ ($0 \leq \gamma \leq 1$). When the hopping is only diagonal between pairs of $|+\rangle$ and $|-\rangle$ states at $\gamma=0$, the pseudospin bands are degenerate, and the density of states has the familiar shape obtained for a simple cubic lattice, with bandwidth $6t$, corresponding to the hopping elements of $\frac{1}{2}t$ [Fig. 1(a)]. Increasing γ removes the degeneracy of the

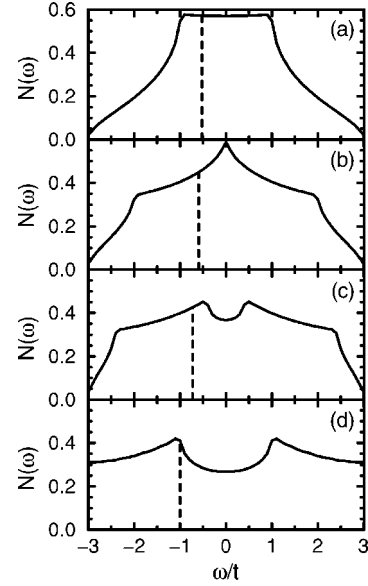


FIG. 1. Evolution of the density of states $N(\omega)$ (in units of $t = 1$) obtained for the tight-binding model (2.9) at $U=0$ with increasing off-diagonal hopping γt : (a) $\gamma=0$, (b) $\gamma=0.5$, (c) $\gamma=1/\sqrt{2}$, and (d) $\gamma=1$; $\gamma=0$ and $\gamma=1$ corresponds to the spin and to the orbital Hubbard model, respectively. Dashed lines show, for the same electron filling $n=0.7$ in all cases, the Fermi energy, which decreases with increasing γ for $n < 1$.

electron bands and gives increasing spectral weight near the band edges without modifying the bandwidth. For genuine e_g electrons (i.e., at $\gamma=1$) the density of states does not start from zero at $\omega = \pm 3t$, as usually for three-dimensional (3D) lattices, but is finite there and has a value close to its average over the entire band [Fig. 1(d)]. Not only is the spectral weight transferred to lower energies, but even the Fermi energy at fixed electron density $n < 1$ decreases with increasing γ , as shown in the example of $n=0.7$ in Fig. 1. Therefore, for a given electron density, at $U=0$ the kinetic energy of e_g electrons (i.e., at $\gamma=1$) is *lower* than in the corresponding spin case (at $\gamma=0$).

Finally, some remarks on the physical interpretation of the orbital Hubbard model are in place here. The first of them concerns electron spin. As said, the electrons in the model are spinless [cf. Eq. (2.1)], which at first sight may seem unphysical. However, such a model is entirely appropriate for real, i.e., spincarrying e_g electrons in a FM state, where the spins are fully polarized. This situation can be realized in a strong magnetic field, or, as in manganites, when the double exchange polarizes the t_{2g} core spins which in turn polarize the e_g band by strong Hund’s rule coupling. Then the spin degrees of freedom are completely frozen out and only the orbital degrees of freedom remain and can contribute to the kinetic energy. Actually, Eq. (2.1) [but with the additional constraint of no double occupancy] is precisely the expression for the kinetic energy of the e_g band in the metallic ferromagnetic phase of the doped manganites $\text{La}_{1-x}\text{A}_x\text{MnO}_3$ (with $\text{A} = \text{Sr}, \text{Ca}, \dots$, and $x \sim 0.3$) when these are described by an extended (orbital-degenerate and large spin) t - J model.¹² So the $U \rightarrow \infty$ limit of the present orbital Hubbard model (2.9) is directly relevant for the physics of

the manganites, and for this reason we will pay extra attention to this limit.

The second remark concerns the parameter γ . As one can readily verify, the kinetic terms in Eq. (2.9) with arbitrary γ are equivalent to the kinetic energy Hamiltonian

$$\hat{H}_t = -\frac{1}{2}t \sum_{\alpha} \sum_{\langle ij \rangle \parallel \alpha} [(1+\gamma)c_{i\xi_{\alpha}}^{\dagger} c_{j\xi_{\alpha}} + (1-\gamma)c_{i\xi_{\alpha}}^{\dagger} c_{j\xi_{\alpha}}], \quad (2.10)$$

which reduces to H_t [Eq. (2.1)] for $\gamma=1$. So, although we have introduced the parameter γ purely as a formal device, it actually describes the relative strength of hopping between the $|\xi_{\alpha}\rangle$ orbitals perpendicular to a bond, and one sees that $\gamma=1$ corresponds to “ ξ -hopping only,” $\gamma=0$ to “ ζ -hopping and ξ -hopping equally strong” (equivalent to the spin case as discussed above), and $\gamma=-1$ to “ ξ -hopping only.” Although such ξ -hopping occurs, for instance, in transition metals as a (*ddd*) element, and is symmetry-allowed in the perovskites, it *cannot* occur by the familiar mechanism of two-step hopping (neither σ -type nor π -type) via a $2p$ orbital on the oxygen ion in between two transition metal ions. It is therefore generally accepted that in physically relevant cases this hopping process is smaller by at least two orders of magnitude than that between $|\zeta_{\alpha}\rangle$ orbitals, and thus, to our knowledge, all work on the manganites has actually been done assuming pure ζ -hopping, i.e., $\gamma=1$. Nevertheless, we will occasionally let γ vary between 0 and 1, not with the intention to suggest that a significant strength of ξ -hopping is actually physically relevant, but rather with the purpose of demonstrating how the pseudospin-nonconserving hopping affects the physical properties of strongly correlated electrons in a partly filled band.

The third remark concerns the difference between real and complex orbitals. It is noteworthy that, unlike in the spin case, already for an individual site there is no spherical symmetry in pseudospin space even at the classical level: the directions available to the pseudospin vector are *not* all physically equivalent. In particular, the real orbitals are spatially anisotropic and have a nonzero diagonal electric quadrupole moment (EQM), $\langle T_i^x \rangle^2 + \langle T_i^y \rangle^2 \neq 0$, whereas the complex orbitals have a cubic shape, with only $\langle T_i^z \rangle \neq 0$. This difference is of course the origin for the hopping Hamiltonian not having $SU(2)$ symmetry. Moreover, as pointed out by Van den Brink and Khomskii,²⁰ in a real compound like a perovskite the EQM couples directly to the lattice, and occupancy of a real orbital would induce a local Jahn-Teller (JT) distortion whereas occupancy of a complex orbital would not.²¹

III. ORBITAL ORDERED STATES

A. Uniform and alternating orbital order

Because the electrons interact by the local Coulomb interaction U , they are prone to instabilities towards *orbital order*, similar to the magnetic instabilities towards spin order in the spin case,²² to which we will compare them. At half-filling ($n=1$) the simplest possibility to reduce the interaction energy $\propto U$ would be to polarize the system completely into *ferro-orbital* (FO) states,

$$|\Phi_{\text{FO}}\rangle = \prod_i c_i^{\dagger}(\psi, \theta)|0\rangle, \quad (3.1)$$

with the pseudospin pointing in the same direction at all sites. As in the spin case, another possibility is *alternating orbital* (AO) order,

$$|\Phi_{\text{AO}}\rangle = \prod_{i \in A} c_i^{\dagger}(\psi_A, \theta_A) \prod_{j \in B} c_j^{\dagger}(\psi_B, \theta_B)|0\rangle, \quad (3.2)$$

with orbitals alternating between two sublattices A and B which cover a cubic lattice. Depending on whether orbitals alternate in every direction, or whether there are lines or planes of ferro-orbital order, these states are classified as G -type (for spin called Néel states), C -type, or A -type AO states. Doubly occupied sites are explicitly avoided in all these states. If the band is partly filled ($n < 1$), these ordered states must of course be modified to involve a coherent mixture of orbital-polarized occupied sites and empty sites. Such fully polarized states are appropriate only in the $U \rightarrow \infty$ limit, where double occupancy is fully suppressed by the Hubbard term and only the kinetic energy, $E_{\text{kin}} = \langle H_t \rangle$, remains relevant.

In contrast to the spin case, where because of the $SU(2)$ symmetry both the FM spin state and the AF spin state are unique, in the present orbital case without $SU(2)$ symmetry there is already a plethora of physically different ordered states even if one does not go beyond two sublattices. In particular, as shown by Takahashi and Shiba,²³ Maezono and Nagaosa,²⁴ Shen *et al.*,²⁵ and particularly stressed by Van den Brink and Khomskii,²⁰ it makes a big difference whether one builds an ordered state completely from complex orbitals (and empty sites) [i.e., $\psi, \psi_A, \psi_B=0, \pi$], leading to what we shall call *complex states*, or whether one uses exclusively real orbitals [i.e., $\psi, \psi_A, \psi_B=\pi/2$], thus constructing *real states*. This can be conveniently demonstrated explicitly by formalizing the description of the $U \rightarrow \infty$ limit by means of the slave fermion formalism, which permits treatment of the general case (i.e., arbitrary ψ 's and θ 's). We present such states here in some detail, since the $U \rightarrow \infty$ limit will serve as a reference in the later discussion.

So we introduce orbital bosons $b_{i\eta}^{\dagger}$ (with $\eta = +, -$) to represent the occupied e_g orbitals, $|\pm\rangle_i = c_{i\pm}^{\dagger}|0\rangle \equiv b_{i\pm}^{\dagger}|\text{vac}\rangle$, and positively charged slave fermions f_i^{\dagger} to represent the empty sites, $|0\rangle_i \equiv f_i^{\dagger}|\text{vac}\rangle$. Thus the original electron operators are replaced according to $c_{i\pm}^{\dagger} = b_{i\pm}^{\dagger} f_i$, and the Hamiltonian takes the form

$$\begin{aligned} \mathcal{H}_{U=\infty} = & +\frac{1}{2}t \sum_{\alpha} \sum_{\langle ij \rangle \parallel \alpha} f_i^{\dagger} f_j [(b_{i+} b_{j+}^{\dagger} + b_{i-} b_{j-}^{\dagger}) \\ & + \gamma (e^{+i\chi_{\alpha}} b_{i+} b_{j-}^{\dagger} + e^{-i\chi_{\alpha}} b_{i-} b_{j+}^{\dagger})], \end{aligned} \quad (3.3)$$

with the local constraint

$$b_{i+}^{\dagger} b_{i+} + b_{i-}^{\dagger} b_{i-} + f_i^{\dagger} f_i = 1, \quad (3.4)$$

implementing the condition of no double occupancy. Orbital order is then imposed by treating the bosons in mean field approximation, i.e., by making the replacements [compare Eq. (2.6)]²⁶

$$\begin{aligned} b_{i+} &\rightarrow \cos(\psi_i/2)e^{-i\theta_i/2}, \\ b_{i-} &\rightarrow \sin(\psi_i/2)e^{+i\theta_i/2}, \end{aligned} \quad (3.5)$$

upon which the local pseudospin operators T_i are given by Eq. (2.7). We are then left with a Hamiltonian describing fermionic holes moving in a background of fixed orbitals.

In the case of FO order the result is explicitly

$$\mathcal{H}_{U=\infty}^{\text{FO}} = +\frac{1}{2}t \sum_{\alpha} \sum_{\langle ij \rangle \parallel \alpha} [1 + \gamma \sin \psi \cos(\theta - \chi_{\alpha})] f_i^{\dagger} f_j. \quad (3.6)$$

Upon Fourier transformation one obtains, reverting to the electron description, a single band with dispersion depending on the orbital angles $\{\psi, \theta\}$,

$$\varepsilon_{U=\infty}^{\text{FO}}(\mathbf{k}) = -t[A_{\mathbf{k}} + \gamma \sin \psi (\cos \theta C_{\mathbf{k}} + \sin \theta D_{\mathbf{k}})], \quad (3.7)$$

where

$$A_{\mathbf{k}} = \cos k_a + \cos k_b + \cos k_c, \quad (3.8)$$

$$C_{\mathbf{k}} = \frac{1}{2}(2 \cos k_c - \cos k_a - \cos k_b), \quad (3.9)$$

$$D_{\mathbf{k}} = \frac{1}{2}\sqrt{3}(\cos k_a - \cos k_b). \quad (3.10)$$

One notes that $C_{\mathbf{k}}$ and $D_{\mathbf{k}}$ transform as the θ and ε components of an E doublet, which makes Eq. (3.7) a cubic invariant (i.e., it does not change under the transformation $\theta \rightarrow \theta - 2\pi/3$ and the simultaneous permutation $k_a \rightarrow k_b \rightarrow k_c \rightarrow k_a$). It will be useful to introduce also

$$P_{\mathbf{k}} = \sum_{\alpha} e^{+i\chi_{\alpha}} \cos k_{\alpha} = C_{\mathbf{k}} + iD_{\mathbf{k}}, \quad (3.11)$$

which gets multiplied by the phasefactor $e^{-i2\pi/3}$ under the permutation $k_a \rightarrow k_b \rightarrow k_c \rightarrow k_a$, as well as the associated amplitude,

$$\begin{aligned} B_{\mathbf{k}} = |P_{\mathbf{k}}| &= \{C_{\mathbf{k}} + D_{\mathbf{k}}\}^{1/2} \\ &= \{\cos^2 k_a + \cos^2 k_b + \cos^2 k_c \\ &\quad - (\cos k_a \cos k_b + \cos k_b \cos k_c \\ &\quad + \cos k_c \cos k_a)\}^{1/2}, \end{aligned} \quad (3.12)$$

which transforms as A_1 , i.e., has cubic symmetry.²⁷

Amongst the various phases with AO order let us consider first those of G -type (Néel-type), denoted by G -AO. One obtains from Eq. (3.3) the two-sublattice Hamiltonian ($i \in A, j \in B$),

$$\begin{aligned} \mathcal{H}_{U=\infty}^{G\text{-AO}} &= \frac{1}{2}t \sum_{\alpha} \sum_{\langle ij \rangle \parallel \alpha} \{[\cos \psi_{-} \cos \theta_{-} - i \cos \psi_{+} \sin \theta_{-}] \\ &\quad + \gamma[\sin \psi_{+} \cos(\theta_{+} - \chi_{\alpha}) + i \sin \psi_{-} \sin(\theta_{+} - \chi_{\alpha})]\} f_i^{\dagger} f_j, \end{aligned} \quad (3.13)$$

depending on the orbital angles $\{\psi_A, \psi_B, \theta_A, \theta_B\}$, for which we introduce the shorthand notation for *half* the intersublattice angles,

$$\psi_{\pm} = \frac{1}{2}(\psi_A \pm \psi_B), \quad \theta_{\pm} = \frac{1}{2}(\theta_A \pm \theta_B). \quad (3.14)$$

Upon Fourier transformation and diagonalization of the resulting 2×2 matrix this yields two electron bands (in the reduced Brillouin zone),

$$\begin{aligned} \varepsilon_{U=\infty, \pm}^{G\text{-AO}}(\mathbf{k}) &= \pm t \{[\cos \psi_{-} \cos \theta_{-} A_{\mathbf{k}} + \gamma \sin \psi_{+} (\cos \theta_{+} C_{\mathbf{k}} \\ &\quad + \sin \theta_{+} D_{\mathbf{k}})]^2 + [\cos \psi_{+} \sin \theta_{-} A_{\mathbf{k}} \\ &\quad - \gamma \sin \psi_{-} (\sin \theta_{+} C_{\mathbf{k}} - \cos \theta_{+} D_{\mathbf{k}})]^2\}^{1/2}. \end{aligned} \quad (3.15)$$

By a similar derivation one may obtain the electronic structure for the A -type and C -type AO phases. Using the same notation as above one finds

$$\begin{aligned} \varepsilon_{U=\infty, \pm}^{A\text{-AO}}(\mathbf{k}) &= t \sum_{\alpha=a,b} \left\{ 1 + \frac{1}{2} \gamma [\sin \psi_A \cos(\theta_A - \chi_{\alpha}) + \sin \psi_B \cos(\theta_B - \chi_{\alpha})] \right\} \cos k_{\alpha} \pm t \left\{ \left(\frac{\gamma}{2} \sum_{\alpha=a,b} [\sin \psi_A \cos(\theta_A - \chi_{\alpha}) \right. \right. \\ &\quad \left. \left. - \sin \psi_B \cos(\theta_B - \chi_{\alpha})] \cos k_{\alpha} \right)^2 + [(\cos \psi_{-} \cos \theta_{-} + \gamma \sin \psi_{+} \cos \theta_{+})^2 + (\cos \psi_{+} \sin \theta_{-} - \gamma \sin \psi_{-} \sin \theta_{+})^2] \cos^2 k_c \right\}^{1/2}, \end{aligned} \quad (3.16)$$

$$\begin{aligned} \varepsilon_{U=\infty, \pm}^{C\text{-AO}}(\mathbf{k}) &= t \left\{ \left(1 + \frac{1}{2} \gamma [\sin \psi_A \cos \theta_A + \sin \psi_B \cos \theta_B] \right) \cos k_c \pm \left[\frac{\gamma}{2} (\sin \psi_A \cos \theta_A - \sin \psi_B \cos \theta_B) \cos k_c \right]^2 \right. \\ &\quad \left. + \left\{ \cos \psi_{-} \cos \theta_{-} (\cos k_a + \cos k_b) + \gamma \sin \psi_{+} \left[\cos \left(\theta_{+} - \frac{2\pi}{3} \right) \cos k_a + \cos \left(\theta_{+} + \frac{2\pi}{3} \right) \cos k_b \right] \right\}^2 \right. \\ &\quad \left. + \left\{ \cos \psi_{+} \sin \theta_{-} (\cos k_a + \cos k_b) - \gamma \sin \psi_{-} \left[\sin \left(\theta_{+} - \frac{2\pi}{3} \right) \cos k_a + \sin \left(\theta_{+} + \frac{2\pi}{3} \right) \cos k_b \right] \right\}^2 \right\}^{1/2}. \end{aligned} \quad (3.17)$$

It is now straightforward to derive from Eqs. (3.7) and (3.15)–(3.17) the dispersion in any particular orbital-ordered phase with either *complex* or *real* orbitals.

For the FOr [$\psi = \pi/2$] and the various AOr [$\psi_A = \psi_B = \pi/2$] *real states* the dispersions are

$$\varepsilon_{U=\infty}^{\text{FOR}}(\mathbf{k}) = -t[A_{\mathbf{k}} + \gamma(\cos \theta C_{\mathbf{k}} + \sin \theta D_{\mathbf{k}})], \quad (3.18)$$

$$\varepsilon_{U=\infty, \pm}^{G\text{-AOr}}(\mathbf{k}) = \pm t[\cos \theta A_{\mathbf{k}} + \gamma(\cos \theta_+ C_{\mathbf{k}} + \sin \theta_+ D_{\mathbf{k}})], \quad (3.19)$$

$$\begin{aligned} \varepsilon_{U=\infty, \pm}^{A\text{-AOr}}(\mathbf{k}) &= \frac{1}{3}t\{(2 - \gamma \cos \theta_+ \cos \theta_-)(A_{\mathbf{k}} - C_{\mathbf{k}}) \\ &+ 3\gamma \sin \theta_+ \cos \theta_- D_{\mathbf{k}} \pm [(\gamma \sin \theta_+ \sin \theta_-)(A_{\mathbf{k}} - C_{\mathbf{k}}) \\ &+ 3\gamma \cos \theta_+ \sin \theta_- D_{\mathbf{k}}]^2 + ((\cos \theta_- + \gamma \cos \theta_+) \\ &\times (A_{\mathbf{k}} + 2C_{\mathbf{k}}))^2\}^{1/2}, \end{aligned} \quad (3.20)$$

$$\begin{aligned} \varepsilon_{U=\infty, \pm}^{C\text{-AOr}}(\mathbf{k}) &= \frac{1}{3}t\{(1 + \gamma \cos \theta_+ \cos \theta_-)(A_{\mathbf{k}} + 2C_{\mathbf{k}}) \\ &\pm [(\gamma \sin \theta_+ \sin \theta_-)(A_{\mathbf{k}} + 2C_{\mathbf{k}})]^2 + ((2 \cos \theta_- \\ &- \gamma \cos \theta_+)(A_{\mathbf{k}} - C_{\mathbf{k}}) + 3\gamma \sin \theta_+ D_{\mathbf{k}})^2\}^{1/2}. \end{aligned} \quad (3.21)$$

In contrast to the complex states discussed below, *all real states*, whether FO or AO of any type and whatever the value of θ (or θ_A and θ_B), *explicitly break cubic symmetry*, i.e., their dispersion is anisotropic. This nonequivalence between real and complex states is a manifestation of the broken $SU(2)$ symmetry in the orbital Hubbard model (2.9). In extreme cases the dispersion is two-dimensional (2D). For instance, the dispersion of the ‘‘antiferro’’ (i.e., with $\mathbf{T}_A = -\mathbf{T}_B$) G -type AO state with alternating $|x\rangle$ and $|z\rangle$ orbitals (G -AOxz) [with $\theta_A = 0$ and $\theta_B = \pi$],

$$\varepsilon_{U=\infty, \pm}^{G\text{-AOxz}}(\mathbf{k}) = \pm \gamma t D_{\mathbf{k}} = \pm \gamma t \frac{\sqrt{3}}{2}(\cos k_a - \cos k_b), \quad (3.22)$$

is 2D because the hopping along the c axis is fully suppressed when $x^2 - y^2$ and $3z^2 - r^2$ orbitals alternate. Similarly, the dispersion of the fully $|x\rangle$ -polarized (FOx) state ($\theta = \pi$),

$$\begin{aligned} \varepsilon_{U=\infty}^{\text{FOx}}(\mathbf{k}) &= -t[A_{\mathbf{k}} - \gamma C_{\mathbf{k}}] = -t\left[\left(1 + \frac{1}{2}\gamma\right)(\cos k_a + \cos k_b) \right. \\ &\left. + (1 - \gamma)\cos k_c\right], \end{aligned} \quad (3.23)$$

becomes 2D in the genuine orbital case ($\gamma = 1$), because when only $x^2 - y^2$ orbitals are occupied, the only type of hopping allowed in this case, i.e., ζ -hopping [see Eq. (2.10)], is suppressed along the c axis.

Other states are also anisotropic but typically have dispersion with contributions due to all three cubic directions. As an example, the dispersion of the G -type AO state with alternating $3x^2 - r^2$ and $3y^2 - r^2$ orbitals ($\theta_A = -\theta_B = -4\pi/3$) along the a and b cubic axes (G -AOab),

$$\begin{aligned} \varepsilon_{U=\infty, \pm}^{G\text{-AOab}}(\mathbf{k}) &= \pm t\left[-\frac{1}{2}A_{\mathbf{k}} + \gamma C_{\mathbf{k}}\right] \\ &= \mp \frac{1}{2}t[(1 + \gamma)(\cos k_a + \cos k_b) \\ &+ (1 - 2\gamma)\cos k_c], \end{aligned} \quad (3.24)$$

is cubic at $\gamma = 0$, but becomes predominantly but not fully 2D for $\gamma = 1$. By contrast, the dispersion of the ($\theta_A = -\theta_B = \pi/2$) state, with alternation between symmetric and antisymmetric combinations, ($|x\rangle + |z\rangle$) and ($|x\rangle - |z\rangle$), called G -AOsa,

$$\begin{aligned} \varepsilon_{U=\infty, \pm}^{G\text{-AOsa}}(\mathbf{k}) &= \pm \gamma t C_{\mathbf{k}} \\ &= \pm \gamma t\left[-\frac{1}{2}(\cos k_a + \cos k_b) + \cos k_c\right], \end{aligned} \quad (3.25)$$

is quasi-one-dimensional (quasi-1D), qualitatively similar to that of the $|z\rangle$ -polarized (FOz) state ($\theta = 0$),

$$\begin{aligned} \varepsilon_{U=\infty}^{\text{FOz}}(\mathbf{k}) &= -t[A_{\mathbf{k}} + \gamma C_{\mathbf{k}}] = -t\left[\left(1 - \frac{1}{2}\gamma\right)(\cos k_a + \cos k_b) \right. \\ &\left. + (1 + \gamma)\cos k_c\right], \end{aligned} \quad (3.26)$$

which becomes quasi-1D in the orbital case ($\gamma = 1$).

The reduced symmetry of the FOx and FOz states is reflected in their respective densities of states, shown in Fig. 2(d), which lead to favorable kinetic energies [see Fig. 3(d)], as discussed in Sec. III B. Obviously, such broken-symmetry states could be favored either in low dimensional systems, as the FOx state found for a 2D square lattice,²⁸ and suggested for bilayer manganites,²⁹ or by a strong JT effect favoring a particular type of occupied e_g orbitals due to oxygen distortions, as realized, for instance, in bilayer systems.³⁰ The latter applies also for the G -type AO states, which have typically smaller bandwidths than the FO states; a few examples are shown in Figs. 2(b) and 2(c).

As illustrative examples of the A -type and C -type phases with alternating real orbitals [either along the c axis or in the (a, b) planes], we give dispersions in each case for: (i) $\theta_A = -\theta_B = \pi/2$, i.e., with alternating $(|x\rangle \pm |z\rangle)/\sqrt{2}$ states, and (ii) $\theta_A = 0$, $\theta_B = \pi$, with alternating $|x\rangle$ and $|z\rangle$ states,

$$\begin{aligned} \varepsilon_{U=\infty, \pm}^{A\text{-AOsa}}(\mathbf{k}) &= \frac{1}{3}t\{2(A_{\mathbf{k}} - C_{\mathbf{k}}) \pm \gamma[(A_{\mathbf{k}} + 2C_{\mathbf{k}})^2 + 9D_{\mathbf{k}}^2]^{1/2}\} \\ &= t\left\{\cos k_a + \cos k_b \pm \gamma\left[\frac{3}{4}(\cos k_a - \cos k_b)^2 \right. \right. \\ &\left. \left. + \cos^2 k_c\right]^{1/2}\right\}, \end{aligned} \quad (3.27)$$

$$\begin{aligned} \varepsilon_{U=\infty, \pm}^{A\text{-AOxz}}(\mathbf{k}) &= \frac{1}{3}t(2 \pm \gamma)(A_{\mathbf{k}} - C_{\mathbf{k}}) \\ &= t\left(1 \pm \frac{1}{2}\gamma\right)(\cos k_a + \cos k_b), \end{aligned} \quad (3.28)$$

$$\begin{aligned} \varepsilon_{U=\infty, \pm}^{C\text{-AOsa}}(\mathbf{k}) &= \frac{1}{3}t[(1 \pm \gamma)A_{\mathbf{k}} + (2 \mp \gamma)C_{\mathbf{k}}] \\ &= t\left[\cos k_c \pm \frac{1}{2}\gamma(\cos k_a + \cos k_b)\right], \end{aligned} \quad (3.29)$$

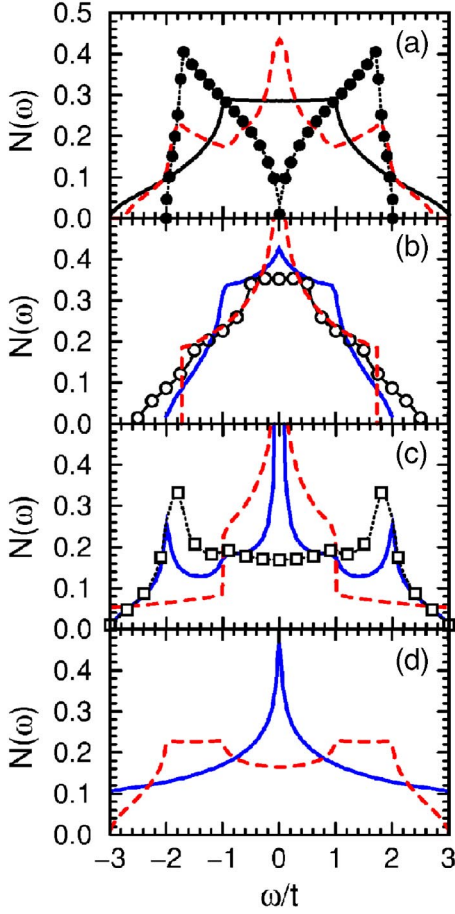


FIG. 2. (Color online) Density of states $N(\omega)$ at $\gamma=1$ (in units of $t=1$) for different orbital ordered phases: (a) complex orbital order: uniform FO+ [degenerate with A-AO \pm] (solid line), G-AO \pm (filled circles), and C-AO \pm (dashed line); (b) alternating real orbital order in G-type phases: G-AO sa (solid line) [the same density of states is obtained for C-AO sa phase], G-AO xz (dashed line), and G-AO ab (circles); (c) alternating real orbital order in selected C- and A-type phases: C-AO xz (solid line), A-AO xz (dashed line), and A-AO sa (squares); and (d) real uniform orbital order FO x (solid line) and FO z (dashed line).

$$\begin{aligned} \varepsilon_{U=\infty, \pm}^{C-AOxz}(\mathbf{k}) &= \frac{1}{3} t \{ A_{\mathbf{k}} + 2C_{\mathbf{k}} \pm \gamma [(A_{\mathbf{k}} + 2C_{\mathbf{k}})^2 + 9D_{\mathbf{k}}^2]^{1/2} \} \\ &= t \left[\cos k_c \pm \gamma \left\{ \frac{3}{4} (\cos k_a - \cos k_b)^2 + \cos^2 k_c \right\}^{1/2} \right]. \end{aligned} \quad (3.30)$$

The anisotropy of these phases is quite strong, and the A-AO xz phase has even a 2D dispersion.

Finally we consider the orbital ordered states with *complex orbitals*. For two of these complex states, namely the ferro $|+\rangle$ -polarized orbital order (FO+) [$\psi=0$] and the G-type alternating orbital order (AO \pm) with $|+\rangle/|-\rangle$ staggered orbitals [with $\psi_A=0$ and $\psi_B=\pi$], all cubic directions are equivalent, and one finds the dispersions

$$\varepsilon_{U=\infty}^{FO+}(\mathbf{k}) = -tA_{\mathbf{k}} \quad (3.31)$$

and

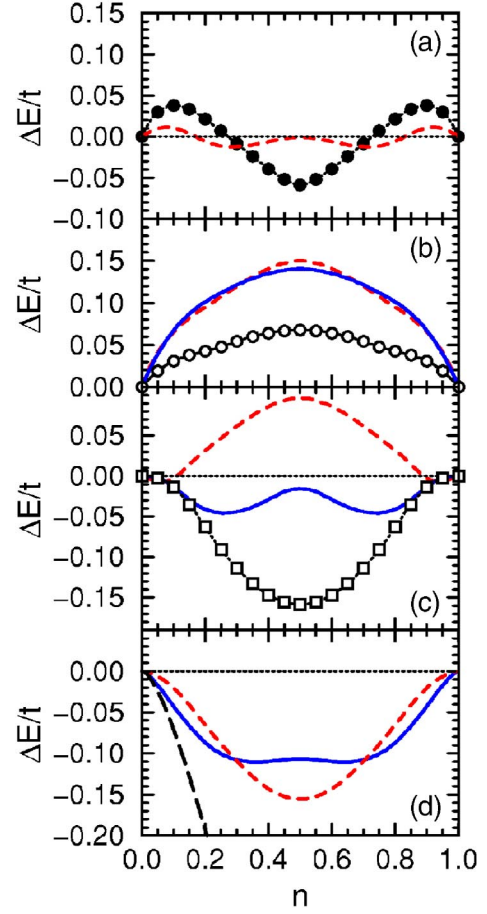


FIG. 3. (Color online) Kinetic energy gain (loss) $\Delta E/t$ with respect to FO+ phase [reference zero energy given by horizontal dotted lines], as a function of electron filling n for various orbital ordered phases (at $U=\infty$): (a) complex orbital order: G-AO \pm (filled circles), and C-AO \pm (dashed line); (b) alternating real orbital order in G-type phases: G-AO sa (solid line) [degenerate with C-AO sa phase], G-AO xz (dashed line), and G-AO ab (circles); (c) alternating real orbital order in selected C- and A-type phases: C-AO xz (solid line), A-AO xz (dashed line), and A-AO sa (squares); and (d) uniform real orbital order FO x (solid line) and FO z (dashed line). The long-dashed line in (d) shows the kinetic energy for noninteracting electrons in the e_g band (disordered phase at $U=0$).

$$\varepsilon_{U=\infty, \pm}^{G-AO\pm}(\mathbf{k}) = \pm \gamma t B_{\mathbf{k}}, \quad (3.32)$$

respectively. Thus one finds that the dispersion of the FO+ state and its density of states, shown in Fig. 2(a), is that of a simple cubic lattice, as it originates entirely from the pseudospin-conserving hopping $\propto c_{i\pm}^\dagger c_{j\pm}$, because at $U \rightarrow \infty$ the alternating, pseudospin-nonconserving, hopping is fully suppressed by the imposed FO+ order. The reverse is true in the G-AO \pm state: here the dispersion $\propto \pm B_{\mathbf{k}}$ comes entirely from the alternating hopping $\propto c_{i\pm}^\dagger c_{j\mp}$, as the pseudospin-conserving hopping is fully suppressed by the AO \pm order. It is an important feature of both these complex states, built from cubic orbitals, that they *retain cubic symmetry*. Precisely for that reason these complex orbital ordered states were proposed as candidates for the ground state of the FM

metallic phase of the manganites^{20,23} to explain the observed cubic symmetry of the magnon spectra.^{31,32}

The other two orbital-ordered complex states break explicitly cubic symmetry: the A -type and C -type AO_{\pm} states. In the A - AO_{\pm} state layers of $|+\rangle$ and $|-\rangle$ orbitals alternate in the c direction, resulting in the dispersion

$$\begin{aligned} \varepsilon_{U=\infty,\pm}^{A-AO_{\pm}}(\mathbf{k}) &= \frac{1}{3}t[(2 \pm \gamma)A_{\mathbf{k}} - 2(1 \mp \gamma)C_{\mathbf{k}}] \\ &= t(\cos k_a + \cos k_b \pm \gamma \cos k_c). \end{aligned} \quad (3.33)$$

This dispersion is qualitatively equivalent to that of the $FO+$ state, and thus the densities of states of the $FO+$ and A - AO_{\pm} phases are the same. The reason is that replacing in the c -direction every second $|+\rangle$ orbital by a $|-\rangle$ orbital does not affect the hopping parameter along c , and so the resulting doubling of the unit cell only halves the Brillouin zone without changing the dispersion. In the C - AO_{\pm} state instead columns of $|+\rangle$ and $|-\rangle$ orbitals alternate in the (a, b) planes, and one finds

$$\begin{aligned} \varepsilon_{U=\infty,\pm}^{C-AO_{\pm}}(\mathbf{k}) &= \frac{1}{3}t\{A_{\mathbf{k}} + 2C_{\mathbf{k}} \pm \gamma[9D_{\mathbf{k}}^2 + (A_{\mathbf{k}} - C_{\mathbf{k}})^2]\} \\ &= t[\cos k_c \pm \gamma(\cos^2 k_a + \cos^2 k_b - \cos k_a \cos k_b)^{1/2}]. \end{aligned} \quad (3.34)$$

In contrast to the $FO+$, G - AO_{\pm} , and A - AO_{\pm} phases, the C - AO_{\pm} phase is not cubic symmetric.

The densities of states of the complex states show a gradual crossover with increasing alternating orbital character from the full bandwidth of $6t$ for the $FO+$ and A - AO_{\pm} phases, obtained also at $U=0$ both for the spin problem and for the e_g band (Fig. 1), to a narrower bandwidth of $2(1 + \sqrt{3})t$ for the C - AO_{\pm} phase, and finally to a bandwidth of $4t$ for the G - AO_{\pm} phase. It is remarkable that, upon going from the $FO+$ phase to the A - AO_{\pm} phase, the change from uniform to alternating orbital order along only one cubic direction does not modify the density of states, while the density of states changes its shape completely upon going to the G - AO_{\pm} phase, with a large spectral weight accumulated now close to the band edges, resulting in a quite peculiar density of states with large maxima close to $|\omega| \approx 2\gamma t$, separated by a minimum with $N(0)=0$ at $\omega=0$ [Fig. 2(a)]. The density of states for the C - AO_{\pm} phase has a width of $2(1 + \sqrt{3})t$, and represents an intermediate case, having some features in common with that of the G - AO_{\pm} phase.

B. Densities of states and kinetic energies in orbital ordered states

It is worthwhile to consider next the densities of states of various orbital ordered states in a little more detail (see Fig. 2), and investigate their consequences for the kinetic energy (Fig. 3). Focusing first on the bandwidth, we note that for any FO state this takes the maximum attainable value $6t$. This result is not limited to the FO states considered explicitly above, i.e., the complex $FO+$ and the real FOz and FOx states, for which it was already pointed out by Van den Brink and Khomskii,²⁰ but holds in general, i.e., for arbitrary ψ and

θ , as readily shown from Eq. (3.7). Moreover, the result is independent of γ and so holds both in the orbital case and in the spin case.

By contrast, in any G -type AO state the bandwidth is smaller than $6t$ [see Fig. 2(b)], and depends on γ . In particular, in any G -type “antiferro” state (with $T_A = -T_B$, so $\psi_B = \pi - \psi_A$ and $\theta_B = \theta_A - \pi$), such as the complex G - AO_{\pm} state or the real G - $AOxz$ and G - $AOsa$ states considered above, the width is proportional to γ (viz. $4\gamma t$, $2\sqrt{3}\gamma t$, and $4\gamma t$, respectively, for those three) as follows from Eq. (3.15). In such a state the bandwidth therefore, correctly, collapses to zero in the spin case ($\gamma=0$) where hopping is completely suppressed by the AF spin order.³³ The important point to note here is that at finite γ , and so in particular in the genuine orbital case, the bandwidth even of an “antiferro” state is *finite* though smaller than that of the FO states. Thus, while in the spin case the kinetic energy of carriers is fully lost when going from FM to Néel-type AF order, this is not so for the analogous FO to G -type AO transition in the orbital case.

One might still be tempted to believe that, as familiar from the spin case, also in the orbital case FO order is most favorable for lowering the kinetic energy of charge carriers, simply because this gives the largest bandwidth. However, the situation is not that simple, not only because there are several inequivalent FO states with different densities of states which have nevertheless the same bandwidth, but also because some A - AO and C - AO phases have again the same bandwidth, and so one really has to consider the details of the density of states in each case. This is demonstrated in Fig. 3, which shows the kinetic energy gain ΔE with respect to the complex $FO+$ state as a function of electron filling n for various FO and AO states with (complex or real) orbital order, obtained by straightforward integration of the respective density of states. Indeed, at small electron filling n , and also at small doping $x=1-n$, ΔE is lower for the (FO , A - AO , and C - AO) states with full bandwidth $6t$ than for any state with a narrower density of states, in particular for the G -type AO states of Fig. 3(b), because the first doped holes enter in the former case with an energy $\sim -3t$ close to the band edge, while the lowest accessible energy is higher in all G - AO states. Note that the orbital order observed in $LaMnO_3$ is close to that of the C - $AOsa$ phase,³⁴ and this phase has the same density of states as the G - $AOsa$ phase [see Fig. 2(b)], and thus has a rather unfavorable kinetic energy [Fig. 3(b)]. This demonstrates that both an interplay between spin and orbital order due to the SE interactions at finite U , and the JT interactions between orbitals on neighboring sites, induced by the coupling to the lattice, play an important role in real materials and stabilize the orbital order observed in undoped $LaMnO_3$.^{6,35}

Among the states with AO order of real orbitals, but FO order along one or two cubic directions, we identified three phases, C - $AOxz$, A - $AOxz$, and A - $AOsa$, which have lower energies than the $FO+$ phase close to $n=0$ and $n=1$ [Fig. 3(c)]. All of them have the full bandwidth $6t$ [Fig. 2(c)], but a finite density of states at $\omega=-3t$ gives the A - $AOxz$ phase the lowest energy of these phases at very low n or x . At somewhat higher filling $n \sim 0.07$ (doping $x \sim 0.07$) the other two phases take over, and are in fact more stable than the $FO+$ phase in the entire regime of n . This follows from the

large densities of states of these phases at $|\omega| \approx 2t$. In contrast, the A -AO xz phase with a large spectral weight close to $\omega=0$ has a higher energy than the FO+ phase in a broad range of electron filling $0.11 < n < 0.89$.

The above discussion shows that at finite but still rather modest electron filling or doping, the overall shape of the density of states becomes more important, and the states with large density of states near the band edges could be favored *a priori*, even in cases when the bandwidth is smaller than $6t$. An interesting example here is the complex ‘‘antiferro’’ G -AO \pm state, with its energy falling below that of the complex FO+ state for $n > 0.27$ or $x > 0.27$ [Fig. 3(a)], because of the large number of states available in the G -AO \pm state just close to the band edges at $|\omega|=2t$, whereas in the FO+ state the energy of available electron states, though initially $-3t$, rises rapidly with increasing doping [Fig. 2(a)]. However, in reality the transition from an FO+ to G -AO \pm state does not happen, as the real FO (FO z and FO x) states have even lower kinetic energy throughout than both complex states. This can be ascribed to the lower-dimensional nature of their dispersion and the resulting different location of the Van Hove singularities, which [compare Fig. 2(d)] enhances the density of states near the band edges at $\pm 3t$ and at the band center for the 2D FO x state, and in the intermediate range $t \lesssim |\omega| \lesssim 2t$ for the quasi-1D FO z state. As a result, at small filling (doping) the kinetic energy gain ΔE is the lowest one for the FO x state, while at larger filling $n \gtrsim 0.30$ (doping $x \gtrsim 0.30$), the FO z state takes over. However, in this regime of electron filling the energy gain ΔE for the A -AO sa phase is lower by a few percent, and the two phases may be considered as practically degenerate.

For comparison and later reference we have included in Fig. 3 also the kinetic energy for the uncorrelated e_g band (the correlated OL phase is analyzed in Sec. V). Of course, at $U=0$ any kind of orbital order is absent and one finds by far the lowest kinetic energy for the disordered e_g orbitals. The e_g bands have then the dispersion given by

$$\varepsilon_{U=0,\pm}(\mathbf{k}) = -t(A_{\mathbf{k}} \pm \gamma B_{\mathbf{k}}). \quad (3.35)$$

Remarkably, these bands at $U=0$ represent formally a superposition of the FO+ and G -AO \pm bands at $U=\infty$,

$$\varepsilon_{U=0,\pm}(\mathbf{k}) = \varepsilon_{U=\infty}^{\text{FO+}}(\mathbf{k}) + \varepsilon_{U=\infty,\pm}^{G\text{-AO}\pm}(\mathbf{k}), \quad (3.36)$$

and so naturally also show full cubic symmetry and a bandwidth equal to $6t$ [Fig. 1(d)]. One notes that, because both pseudospin-conserving and pseudospin-nonconserving hopping channels fully contribute here, considerably more kinetic energy can be gained than in any of the orbital-ordered states. In particular, as Fig. 1(d) shows, there is a large density of states at and near the band edges, and thus ΔE is the lowest in this disordered state already at small electron filling n , and then remains so throughout. Of course, this large kinetic energy gain will be partly lost for large U near $n=1$, where at least one hopping channel gets partially suppressed by electron correlations. However, the result here indicates that the tendency towards the OL state with disordered e_g orbitals is particularly pronounced. We shall come back to this point, presenting more evidence in favor of the correlated OL phase, in Sec. V.

IV. HARTREE-FOCK APPROXIMATION

A. Instabilities towards orbital order

We turn now to the orbital Hubbard model (2.9) with finite U , where it is to be expected that polarization, when it occurs, need not be complete but can be partial, as in the spin case. Also, the existence of orbital ordered states will in general require a sufficiently large U/t . Which instabilities towards orbital ordering occur and at what value of U/t can be investigated either by considering the corresponding susceptibilities, e.g., in random phase approximation,²³ or by comparing the energies determined in the HF approximation.²⁰ If various ordered states are possible, one needs to calculate their energy (or free energy at finite temperature) to determine which one is actually realized.

In the absence of $SU(2)$ symmetry it is not sufficient to decouple the interaction term in Eq. (2.9) in the familiar mean-field way, $n_{i+}n_{i-} \approx (\langle n_{i+} \rangle n_{i-} + n_{i+} \langle n_{i-} \rangle - \langle n_{i+} \rangle \langle n_{i-} \rangle)$, but one needs instead the general HF decoupling,

$$n_{i+}n_{i-} \approx (\langle n_{i+} \rangle n_{i-} + n_{i+} \langle n_{i-} \rangle - \langle n_{i+} \rangle \langle n_{i-} \rangle) - (\langle T_i^+ \rangle c_{i-}^\dagger c_{i+} + c_{i+}^\dagger c_{i-} \langle T_i^- \rangle - \langle T_i^+ \rangle \langle T_i^- \rangle). \quad (4.1)$$

In the FO case, i.e., when one assumes a single three-component order parameter, $T_z = \langle T_i^z \rangle$, $T_+ = \langle T_i^+ \rangle$, $T_- = \langle T_i^- \rangle$, one obtains upon Fourier transformation the HF Hamiltonian

$$H_{\text{HF}}^{\text{FO}} = \sum_{\mathbf{k}} (c_{\mathbf{k}+}^\dagger c_{\mathbf{k}-}^\dagger) \begin{pmatrix} \frac{1}{2}Un - UT_z - tA_{\mathbf{k}} & -UT_- - \gamma tP_{\mathbf{k}}^* \\ -UT_+ - \gamma tP_{\mathbf{k}} & \frac{1}{2}Un + UT_z - tA_{\mathbf{k}} \end{pmatrix} \times \begin{pmatrix} c_{\mathbf{k}+} \\ c_{\mathbf{k}-} \end{pmatrix} - \frac{1}{4}Un^2 + U(T_z^2 + T_+T_-), \quad (4.2)$$

with $P_{\mathbf{k}}$ given by Eq. (3.11). The eigenvalues are (with $T_+ = Te^{i\theta}$, $T_- = Te^{-i\theta}$, so that $T_+T_- = T^2 = T_x^2 + T_y^2$)

$$\varepsilon_{\pm}^{\text{FO}}(\mathbf{k}) = -tA_{\mathbf{k}} + U\left(\frac{1}{2}n \pm \hat{E}_{\mathbf{k}}\right), \quad (4.3)$$

where

$$\hat{E}_{\mathbf{k}} = \left[T^2 + T_z^2 + 2\frac{\gamma t}{U}T(\cos \theta C_{\mathbf{k}} + \sin \theta D_{\mathbf{k}}) + \left(\frac{\gamma t}{U}\right)^2 B_{\mathbf{k}}^2 \right]^{1/2}, \quad (4.4)$$

and the HF groundstate energy per site is then given by

$$E_{\text{HF}}^{\text{FO}} = \frac{1}{N} \sum_{\mathbf{k}} [n_-(\mathbf{k})\varepsilon_-^{\text{FO}}(\mathbf{k}) + n_+(\mathbf{k})\varepsilon_+^{\text{FO}}(\mathbf{k})] - \frac{1}{4}Un^2 + U(T^2 + T_z^2), \quad (4.5)$$

where $n_-(\mathbf{k})$ [$n_+(\mathbf{k})$] is the occupation number of the lower (upper) band. For large U ($\gtrsim 6t$) a gap opens, and so for less than half-filling only the lower band is occupied. Setting the derivatives of $E_{\text{HF}}^{\text{FO}}$ with respect to n , T_z , T , and θ equal to zero then yields the self-consistency equations

$$n = \frac{1}{N} \sum_{\mathbf{k}} n_-(\mathbf{k}), \quad (4.6)$$

$$T_z = \frac{1}{2N} \sum_{\mathbf{k}} n_{-}(\mathbf{k}) \frac{T_z}{\hat{E}_{\mathbf{k}}}, \quad (4.7)$$

$$T = \frac{1}{2N} \sum_{\mathbf{k}} n_{-}(\mathbf{k}) \frac{T + \frac{\gamma}{U} (\cos \theta C_{\mathbf{k}} + \sin \theta D_{\mathbf{k}})}{\hat{E}_{\mathbf{k}}}, \quad (4.8)$$

$$0 = \frac{1}{2N} \sum_{\mathbf{k}} n_{-}(\mathbf{k}) \frac{T(\sin \theta C_{\mathbf{k}} - \cos \theta D_{\mathbf{k}})}{\hat{E}_{\mathbf{k}}}. \quad (4.9)$$

While Eq. (4.6) is trivially satisfied in the sense that it simply fixes the Fermi level for given filling n , two general conclusions can be proven from the remaining three equations. Firstly, it follows from Eq. (4.9), because of the dependence of $\hat{E}_{\mathbf{k}}$ on $C_{\mathbf{k}}$ and $D_{\mathbf{k}}$ [see Eq. (4.4)] and the explicit form of

the latter two functions [see Eqs. (3.9) and (3.10)], that for nonzero T the azimuth θ must equal either 0 (or equivalently $+2\pi/3$ or $-2\pi/3$) or π (or equivalently $-\pi/3$ or $+\pi/3$), i.e., the projection of the order parameter on the “real” equatorial plane has to be along one of the cubic directions. Secondly, it follows that both a purely complex state (i.e., $T=0$, $T_z \neq 0$) and a purely real state (i.e., $T_z=0$, $T \neq 0$) are permissible states, in the sense that $T_z=0$ is a self-consistent solution of Eq. (4.7) and alternatively $T=0$ is one of Eq. (4.8). We remark that both these properties of the possible states need not be postulated or assumed but are proven here from the HF self-consistency equations.

As C -type and A -type AO phases would give qualitatively similar results, we will consider from now on only G -type AO phases, and denote them for brevity by “AO” instead of by “ G -AO.” So we assume independent three-component order parameters on interlacing sublattices A and B, $T_z^A = \langle T_i^z \rangle_A$, $T_z^B = \langle T_i^z \rangle_B$, etc. Then the HF Hamiltonian is

$$H_{\text{HF}}^{\text{AO}} = \sum_{\mathbf{k}} \begin{pmatrix} c_{\text{A},\mathbf{k}+}^{\dagger} \\ c_{\text{A},\mathbf{k}-}^{\dagger} \\ c_{\text{B},\mathbf{k}+}^{\dagger} \\ c_{\text{B},\mathbf{k}-}^{\dagger} \end{pmatrix}^T \begin{pmatrix} \frac{1}{2}Un - UT_z^A & -UT_-^A & -tA_{\mathbf{k}} & -\gamma t P_{\mathbf{k}}^* \\ -UT_+^A & \frac{1}{2}Un + UT_z^A & -\gamma t P_{\mathbf{k}} & -tA_{\mathbf{k}} \\ -tA_{\mathbf{k}} & -\gamma t P_{\mathbf{k}}^* & \frac{1}{2}Un - UT_z^B & -UT_-^B \\ -\gamma t P_{\mathbf{k}} & -tA_{\mathbf{k}} & -UT_+^B & \frac{1}{2}Un + UT_z^B \end{pmatrix} \begin{pmatrix} c_{\text{A},\mathbf{k}+} \\ c_{\text{A},\mathbf{k}-} \\ c_{\text{B},\mathbf{k}+} \\ c_{\text{B},\mathbf{k}-} \end{pmatrix} - \frac{1}{4}Un^2 + \frac{1}{2}U[(T_z^A)^2 + T_+^A T_-^A + (T_z^B)^2 + T_+^B T_-^B]. \quad (4.10)$$

Like above, the HF groundstate energy per site is then formally given (with $T_+^A = T^A e^{i\theta_A}$, etc.) by

$$E_{\text{HF}}^{\text{AO}} = \frac{1}{N} \sum_{\beta=1}^4 \sum_{\mathbf{k}} n_{\beta}(\mathbf{k}) \varepsilon_{\beta}^{\text{AO}}(\mathbf{k}) - \frac{1}{4}Un^2 + \frac{1}{2}U[(T^A)^2 + (T_z^A)^2 + (T^B)^2 + (T_z^B)^2], \quad (4.11)$$

where the sum on β is over the four bands and that on \mathbf{k} is over the reduced Brillouin zone. However, as the 4×4 matrix in Eq. (4.11) cannot be diagonalized analytically in the general case (i.e., for arbitrary order parameters), no further progress can be made like in the FO case. In particular one cannot strictly prove that purely real or purely complex states are permissible solutions.

Yet this still seems likely, and if one makes this assumption, then for the case of the complex (AOc) state, i.e., with $T^A = T^B = 0$, the 4×4 matrix simplifies enough to obtain explicit expressions for the band dispersions,

$$\varepsilon_{\beta}^{\text{AOc}}(\mathbf{k}) = +U \left(\frac{1}{2}n \pm \hat{F}_{1,\mathbf{k}} \pm \hat{F}_{2,\mathbf{k}} \right), \quad (4.12)$$

where

$$\hat{F}_{1,\mathbf{k}} = \left[\left(\frac{T_z^A + T_z^B}{2} \right)^2 + \left(\frac{\gamma}{U} B_{\mathbf{k}}^2 \right)^2 \right]^{1/2}, \quad (4.13)$$

$$\hat{F}_{2,\mathbf{k}} = \left[\left(\frac{T_z^A - T_z^B}{2} \right)^2 + \left(\frac{t}{U} \right)^2 A_{\mathbf{k}}^2 \right]^{1/2}. \quad (4.14)$$

Setting the derivatives of $E_{\text{HF}}^{\text{AOc}}$ with respect to n , T_z^A and T_z^B to zero yields again HF self-consistency equations. From these one easily proves that $T_z^A = -T_z^B$, i.e., that the stable complex state is actually the AO \pm state.

For the case of a real (AO r) state, i.e., with $T_z^A = T_z^B = 0$, an analytic solution is also possible, but this is so unwieldy as to be impractical. However, if one further assumes that $T^A = T^B \equiv T$ one can derive the approximate expressions

$$\varepsilon_{\beta}^{\text{AO}r}(\mathbf{k}) = \pm t [A_{\mathbf{k}} \cos \theta_{-} + \gamma (C_{\mathbf{k}} \cos \theta_{+} + D_{\mathbf{k}} \sin \theta_{+})] + U \left(\frac{1}{2}n \pm \hat{G}_{\mathbf{k}} \right), \quad (4.15)$$

where

$$\hat{G}_{\mathbf{k}} = \left[T^2 + \left(\frac{t}{U} \right)^2 \{ A_{\mathbf{k}}^2 \sin^2 \theta_{-} + \gamma^2 (C_{\mathbf{k}} \sin \theta_{+} - D_{\mathbf{k}} \cos \theta_{+})^2 \} \right]^{1/2}, \quad (4.16)$$

valid in the large U limit ($U/t \gg 1$), and again obtain analytic self-consistency equations by taking the derivatives of $E^{\text{AO}r}$ with respect to n , T , θ_{+} , and θ_{-} . From the latter two one can now prove the following. First, that $\theta_{+} = 0$, i.e., $\theta_A = -\theta_B$, so

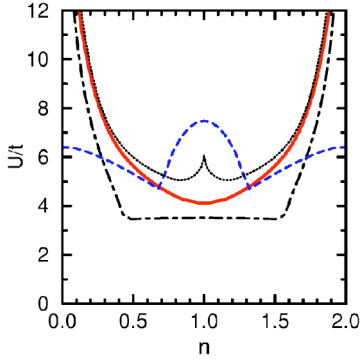


FIG. 4. (Color online) Stoner instability towards FO+ partly polarized states (full line) as a function of band filling n in the orbital Hubbard model ($\gamma=1$), and the inverse of the e_g density of states of Fig. 1(d) (dotted line); full polarization occurs only in the limit $U=\infty$. For the spin model ($\gamma=0$), the corresponding Stoner instability (dashed-dotted line) is given by the inverse of the density of states shown in Fig. 1(a), while saturated FM states occur above the dashed line.

the pseudospin vectors on the two sublattices are mirror images of one another with respect to the cubic direction $\theta=0$ (or the equivalent ones $\theta=\pm 2\pi/3$). Second, that $\cos \theta_\perp \approx -(U/3t)x$ for $x \ll t/U$, i.e., $\theta_A \approx \pi/2 + (U/3t)x$, so that at zero doping the stable solution is the AO s_a state, and with increasing doping the pseudospin vectors tilt slightly away from the cubic direction, making the solution gradually resemble more the AO ab state.³⁶

As an example of the HF instability at intermediate U we have investigated how the complex FO+ (or the equivalent FO-) state develops when U increases, using Eqs. (4.2) and (4.5). First, at $\gamma=0$ one recovers the Stoner criterion $U_\sigma N(E_F)=1$ for the onset of the FM order with increasing U , with the FM saturated states becoming stable at a still larger but finite value of U (Fig. 4). By contrast, in the orbital model at $\gamma=1$ the instability is qualitatively different, and the FO+ (FO-) state appears as a *global property* of the band rather than as an instability at the Fermi surface. The instability occurs at higher values of U for any filling than in the spin case—actually the value of the critical U is very close to that giving full magnetic polarization in the spin case.

Here, unlike in the spin case, the FO order implies that the electronic bands are changed—they develop an additional splitting above a critical value of U , which modifies the shape of the bands and leads to a finite order parameter $T_z = \langle T_z^\pm \rangle \neq 0$. This mechanism of the instability resembles that known in the spin case for the onset of antiferromagnetism. The critical value of U above which weak order appears has therefore no relation to the actual shape of the density of states (see Fig. 4).

We decided not to investigate the phase diagram of the orbital Hubbard model in the HF approximation in detail. Instead, we concentrate first on the qualitatively novel aspects of various possible ordered states in the regime of large U , where, as we will see, the contrast with the spin case manifests itself in the most transparent way. Using these results, we will then comment of the HF phase diagrams analyzed in detail by several groups,^{20,23,24} in Sec. IV D.

B. Superexchange in the complex orbital states

We have already seen that the analysis of the orbital-ordered states simplifies when the splitting of the quasiparticle bands $\propto UT_z$ or $\propto UT$ is sufficiently large that it opens up a gap and only the lower band (lowest two bands for AO order) is (are) partly occupied when $n \leq 1$. It is then straightforward to calculate the energy and the order parameter by summing over the occupied states.

Consider first the ordered states with complex orbitals. In the case of the FO+ state the equation for the order parameter, from Eqs. (4.8) and (4.4), takes the simple form (because only $T_z \neq 0$, while $T=0$):

$$T_z = \frac{1}{2N} \sum_{\mathbf{k}} \frac{n_-(\mathbf{k})}{E_{\mathbf{k}}}, \quad (4.17)$$

$$E_{\mathbf{k}} = \left[1 + \left(\frac{\gamma t}{UT_z} \right)^2 B_{\mathbf{k}}^2 \right]^{1/2}. \quad (4.18)$$

Equation (4.18) shows explicitly that, unlike in the spin case, $T_z=n/2$ only at $U=\infty$, basically because the saturated FO+ state is *not an eigenstate* of the orbital Hubbard model given by Eq. (2.9). Thus the FO+ state is again seen to resemble the AF phase in the spin model.

Similarly, in the AO \pm phase for large enough U the order parameter is given by

$$T_z = \frac{1}{2N} \sum_{\mathbf{k}} \frac{n_1(\mathbf{k}) + n_2(\mathbf{k})}{F_{\mathbf{k}}}, \quad (4.19)$$

$$F_{\mathbf{k}} = \left[1 + \left(\frac{t}{UT_z} \right)^2 A_{\mathbf{k}}^2 \right]^{1/2}, \quad (4.20)$$

rather similar to the FO+ case (4.18), but with the interchange $A_{\mathbf{k}} \leftrightarrow \gamma B_{\mathbf{k}}$. The reason is readily recognized from Eq. (2.9): for FO+ order, the diagonal hopping $\propto c_{i\pm}^\dagger c_{j\pm}$ that gives $A_{\mathbf{k}}$ is order-preserving, while the off-diagonal terms $\propto c_{i\pm}^\dagger c_{j\mp}$ that produce $B_{\mathbf{k}}$ are order-perturbing and reduce T_z . For AO \pm order this is reversed: the off-diagonal hopping $\propto \gamma$ that gives $B_{\mathbf{k}}$ is compatible with the order, while the diagonal one that gives $A_{\mathbf{k}}$ disturbs it.

The similarity between the FO+ and AO \pm states at $\gamma=1$ becomes even more transparent at large U (i.e., $\gg t$), where near half-filling (i.e., for small $x=1-n>0$), upon expansion up to first order in t/U ,

$$T_z^{\text{FO}+} = \frac{1}{2} \left\{ (1-x) - \frac{3\gamma^2}{(1-x)^2} \left(\frac{t}{U} \right)^2 \right\}, \quad (4.21)$$

$$T_z^{\text{AO}\pm} = \frac{1}{2} \left\{ (1-x) - \frac{3-2x}{(1-x)^2} \left(\frac{t}{U} \right)^2 \right\}. \quad (4.22)$$

Note that a SE contribution $\propto (\gamma t)^2/U$ appears also in the FO+ state because the off-diagonal hopping permits virtual charge fluctuations. This result is again qualitatively different from the spin case, where the SE contributes only in the AF states, and so destabilizes uniform FM spin order. In the genuine orbital case ($\gamma=1$) the reduction of the order parameter by SE is the same for FO+ and AO \pm at $x=0$, but at x

≥ 0 it is slightly larger for the FO+ phase. The corresponding expressions for the energy, up to second order in t/U , become

$$E^{\text{FO}^+} = -t \frac{1}{N} \sum_{\mathbf{k}} n_{-}(\mathbf{k}) A_{\mathbf{k}} - \frac{3\gamma^2}{2(1-x)} \frac{t^2}{U}, \quad (4.23)$$

$$E^{\text{AO}^{\pm}} = -\gamma t \frac{1}{N} \sum_{\mathbf{k}} [n_1(\mathbf{k}) - n_2(\mathbf{k})] B_{\mathbf{k}} - \frac{3-2x}{2(1-x)} \frac{t^2}{U}. \quad (4.24)$$

Both are seen to be composed of the $U=\infty$ kinetic energy [compare Eqs. (3.31) and (3.32) for the dispersions] and a (negative) SE energy. Surprisingly, near half-filling the energy per site of the FO phase is *lower* than that of the AO phase at any value of U , not only because the FO phase gains more kinetic energy $\propto -3tx$ than the AO phase $\propto -2tx$, but also because it has lower SE energy. Instead, AO^{\pm} order yields lower energy at larger doping $x \geq 0.27$ as a consequence of its peculiar density of states [Fig. 2(a)].^{23,24} Note that this is *opposite* to the spin case ($\gamma=0$), where the Néel (AF) state has lower energy near $n=1$ and the FM state takes over only above a critical doping $x_c \approx t/2U$.

We emphasize that we have compared as yet only the two complex states with one another, with the express purpose of contrasting the behavior of these orbital states with that of the corresponding spin states. To establish what the most stable orbital-ordered state is, we still have to consider the real states.

C. Superexchange in the real orbital states

The results obtained for the ordered phases with real orbitals are qualitatively similar. We focus here on the representative cases of the FO_x , the FO_z , and the (G -type) AO_{sa} states, which we have shown in Sec. IV to be solutions of the HF equations. Note that the AO_{sa} phase is representative for G -type AO order. For simplicity we ignore here the small higher order correction to the equations below,³⁷ which occur when the actual occupied orbitals deviate from those of the AO_{sa} state towards those pertaining to the AO_{ab} state as discussed above.

At large U/t one finds near half-filling for the order parameters

$$T^{\text{FO}_x(z)} = \frac{1}{2} \left\{ (1-x) - \frac{3\gamma^2}{2(1-x)^2} \left(\frac{t}{U} \right)^2 \right\}, \quad (4.25)$$

$$T^{\text{AO}_{sa}} = \frac{1}{2} \left\{ (1-x) - \frac{6-4x+3\gamma^2}{2(1-x)^2} \left(\frac{t}{U} \right)^2 \right\}. \quad (4.26)$$

The corresponding energies in these ordered phases are

$$E^{\text{FO}_x} = -t \frac{1}{N} \sum_{\mathbf{k}} n_{-}(\mathbf{k}) (A_{\mathbf{k}} - \gamma C_{\mathbf{k}}) - \frac{3\gamma^2}{4(1-x)} \frac{t^2}{U}, \quad (4.27)$$

$$E^{\text{FO}_z} = -t \frac{1}{N} \sum_{\mathbf{k}} n_{-}(\mathbf{k}) (A_{\mathbf{k}} + \gamma C_{\mathbf{k}}) - \frac{3\gamma^2}{4(1-x)} \frac{t^2}{U}, \quad (4.28)$$

$$E^{\text{AO}_{sa}} = -t \frac{1}{N} \sum_{\mathbf{k}} [(n_1(\mathbf{k}) - n_2(\mathbf{k}))] \gamma C_{\mathbf{k}} - \frac{6-4x+3\gamma^2}{4(1-x)} \frac{t^2}{U}. \quad (4.29)$$

Unlike the complex states, the real states are seen not to be degenerate in the undoped case $x=0$. The AO_{sa} state has the lowest energy here, even though the SE contributes also in the FO states. However, we find the same qualitative difference with the familiar AF and FM states for spin order as we found for the complex orbital states—again the SE contributes both in FO and in AO states.

Finally, we remark that the SE contributes also in any other phase, either with mixed FO and AO order (e.g., in the C -AO and A -AO phases of Sec. III), or in a disordered OL state. Depending on whether the occupied orbitals on a given bond are identical or not, virtual processes due to pseudospin-nonconserving or pseudospin-conserving hopping contribute, and we have verified that qualitatively similar results are then obtained to those presented in Eqs. (4.25)–(4.29) above. Such terms would play a role in the low-doping regime and would deserve a separate study in order to establish the phase diagram of weakly doped manganites. Note that in that regime also the spin-dependent SE plays a prominent role, and the present orbital Hubbard model (2.9), which implicitly assumes FM order, becomes insufficient to describe the physical properties of the real materials. On the other hand, the SE terms, being all $\propto t^2/U$, vanish in the limit of large U which we consider in Sec. V, and hence they have no consequences for the stability of the OL phase at $U=\infty$.

D. Qualitative understanding of the Hartree-Fock phase diagram

Finally, let us analyze the possible instabilities of the orbital Hubbard model (2.9) in the HF approximation. In the large U limit relevant for such instabilities, the total energy consists of the kinetic energy at $U=\infty$, discussed in Sec. III A, and a negative SE energy. While we do not intend to make a quantitative comparison between the various phases stable in the HF approximation, knowing that they are anyway destabilized by the correlation effects (see Sec. V), this now enables us to get a simple interpretation of the HF phase diagram of the genuine e_g orbital model ($\gamma=1$),^{20,23–25} using the large U expansion. These earlier HF studies have shown that at half-filling, and in the regime of small doping, for $U > 6t$ the most stable state is the real “antiferro” orbital state, with the orbitals close to those found in the AO_{sa} phase. In this regime the SE energy dominates, and indeed the largest energy gain is then given by Eq. (4.29). At increasing hole doping, however, the kinetic energy of holes moving in the FO_x background is much lower than that in the AO_{sa} phase (see Fig. 3), leading to a transition to “ferro” orbital states when the difference between the SE terms $\propto t^2/U$ is overcome by the difference between the kinetic energies of these two phases. The region of the AO_{sa} phase in the phase diagram decreases when the SE gradually loses its importance with increasing U , as shown by the numerical result of Van den Brink and Khomskii.²⁰

At $U=\infty$ the FO r order is found in the HF approximation at any doping $x>0$. However, at large but finite U the SE is larger in the FO+ than in either FO x or FO z phase, while the difference in the kinetic energy is small [Fig. 3(d)], and thus the FO+ state is the first stable “ferro” state at intermediate values of $8<U/t<12$ and $x\approx 0.15$. However, when x increases further, the kinetic energy difference between the FO x and FO+ phase dominates, and the orbital order changes to FO x . As the SE energy of the two real FO x and FO z states [see Eqs. (4.27) and (4.28)] is the same, the difference in the kinetic energy gives a second transition from the FO x to the FO z phase with increasing x . At small and intermediate $U/t<12$ one finds eventually at $x\sim 0.5$ the AO \pm phase,²⁰ which is stabilized in this regime by a combined effect of large SE energy gain and low kinetic energy (see Fig. 3) which follows from the peculiar density of states of this phase.

In a 2D model the phase diagram is quite different³⁸ and is dominated by the generic tendency towards x^2-y^2 polarization within an (a,b) plane.²⁸ The AO order is then followed by the FO x phase above a critical doping, which decreases with increasing U/t . We note that the region of the FO x phase is enlarged by the offdiagonal hopping terms $\propto \gamma t$,³⁸ in agreement with the above observation that these terms stabilize the FO phases at finite U due to the respective SE energy contributions.

V. ORBITAL LIQUID STATE

A. Kotliar-Ruckenstein slave boson representation

To understand further the essential differences between orbital and spin physics, we develop now an approximate description of the correlated OL disordered state. This is of crucial importance as the HF approximation permits only a comparison of ordered states with one another, and therefore does not allow one to draw any conclusions concerning the stability of the orbital-ordered states with respect to disordered states. This is well-known from spin models—for instance, the FM states in the 2D Hubbard model are stable only in a narrow range of doping $x<0.29$ near half-filling,³⁹ while the HF approximation predicts FM to be stable at any electron filling n .

We will argue below that indeed orbital (FO or AO) order is not robust at $\gamma=1$ and gets replaced by a disordered (OL) phase, if one goes *beyond* the HF approximation and includes electron correlation effects. As we have already seen, the orbital problem is richer than the spin case, as various ordered states are nonequivalent when the $SU(2)$ symmetry is absent. Therefore we shall consider only the limit of very strong correlations and investigate the stability of orbital order specifically in the $U=\infty$ limit, where the OL competes with fully saturated FO [see Eqs. (4.21) and (4.25)] and AO [see Eqs. (4.22) and (4.26)] states.

In order to obtain a reliable variational method to calculate the correlation energy, we have followed the slave boson approach introduced by Kotliar and Ruckenstein¹⁴ for the spin Hubbard model and have adapted it to the orbital case. In this approach the Fock space is enlarged by the introduction of three auxiliary bosons at each site, one for each local

configuration, viz. b_{i+} and b_{i-} associated with the single-occupancy configurations $|i+\rangle$ and $|i-\rangle$, and e_i with the empty configuration $|i0\rangle$ (double occupancy is excluded at $U=\infty$). Then a physical fermion (electron) c is represented by a pseudofermion f and two accompanying bosons according to an expression like $c_{i\beta}^\dagger = f_{i\beta}^\dagger b_{i\beta}^\dagger e_i$, where the two bosons keep track of the change of the local configuration when an electron is added.¹⁴ This construction, however, must preserve the cubic symmetry of the Hamiltonian (2.9), implying that it has to be gauge invariant with respect to those $U(1)$ rotations in orbital space that correspond to a permutation of the cubic axes. The relevant rotation operator is, for arbitrary rotation angle θ ,

$$\hat{U}_i(\theta) = \exp(-i\theta T_i^\dagger). \quad (5.1)$$

The complex orbitals pick up just a phase factor under any rotation of this form, and the operators $\{c_{i+}^\dagger, c_{i-}^\dagger\}$ transform as

$$\begin{aligned} \hat{U}_i(\theta) c_{i+}^\dagger \hat{U}_i^\dagger(\theta) &= e^{-i\theta/2} c_{i+}^\dagger, \\ \hat{U}_i(\theta) c_{i-}^\dagger \hat{U}_i^\dagger(\theta) &= e^{+i\theta/2} c_{i-}^\dagger. \end{aligned} \quad (5.2)$$

As already indicated in Sec. II, the orbital Hubbard Hamiltonian (2.9) is invariant under a uniform rotation at all sites, if the common rotation angle θ is one of the three cubic angles $-4\pi/3$, $+4\pi/3$, 0 , and if this is accompanied by a corresponding shift of the “gauge angles” χ_α by $-2\pi/3$, $+2\pi/3$, 0 , respectively. Actually the diagonal hopping terms in Eq. (2.9) are invariant under the $U(1)$ transformation (5.1) even for arbitrary θ , as a consequence of the $SU(2)$ symmetry of the spin Hubbard model, while the off-diagonal hopping terms pick up phase factors,

$$\begin{aligned} c_{i+}^\dagger c_{j-} &\mapsto e^{-i\theta} c_{i+}^\dagger c_{j-}, \\ c_{i-}^\dagger c_{j+} &\mapsto e^{+i\theta} c_{i-}^\dagger c_{j+}, \end{aligned} \quad (5.3)$$

which get compensated by the shift of the χ_α if θ is a cubic angle. As the three cubic-angle transformations amount to a forward and to a backward simultaneous cyclic permutation of axes and orbitals and to the identity, respectively, the invariance expresses the cubic symmetry of the Hamiltonian.

Therefore we take the slave boson representation as

$$c_{i\pm}^\dagger = b_{i\pm}^\dagger f_{i\pm}^\dagger e_i, \quad (5.4)$$

corresponding to a representation of the local states by

$$\begin{aligned} |i0\rangle &= e_i^\dagger |\text{vac}\rangle, \\ |i+\rangle &= c_{i+}^\dagger |i0\rangle = b_{i+}^\dagger f_{i-}^\dagger |\text{vac}\rangle, \\ |i-\rangle &= c_{i-}^\dagger |i0\rangle = b_{i-}^\dagger f_{i+}^\dagger |\text{vac}\rangle, \end{aligned} \quad (5.5)$$

and we *impose* that the boson and pseudofermion operators transform under $U(1)$ rotations⁴⁰ as

$$\begin{aligned} \hat{U}_i(\theta) e_i^\dagger \hat{U}_i^\dagger(\theta) &= e_i^\dagger, \\ \hat{U}_i(\theta) b_{i\pm}^\dagger \hat{U}_i^\dagger(\theta) &= e^{\mp i\theta} b_{i\pm}^\dagger, \end{aligned}$$

$$\hat{U}_i(\theta) f_{i\pm}^\dagger \hat{U}_i^\dagger(\theta) = e^{\mp i\theta/2} f_{i\pm}^\dagger. \quad (5.6)$$

Note that the phase of the boson operators $b_{i\pm}^\dagger$ changes twice as fast as the phase of the pseudofermion operators $f_{i\pm}^\dagger$, i.e., the bosons have pseudospin $T=1$, while the (pseudo)fermions belong to $T=1/2$. This property guarantees that the $U(1)$ rotation behavior of the electron operators, as given in Eqs. (5.2), is correctly reproduced by the transformation (5.4). Thus the present formulation is indeed gauge invariant and preserves the cubic symmetry of the orbital problem, like the $SU(2)$ -invariant formulation introduced by Frésard and Wölfle preserves the full rotational symmetry for the spin system.⁴¹ Clearly, the construction of a gauge invariant formulation is greatly facilitated by our use of the complex-orbital representation, but a similarly gauge invariant representation in terms of real operators can also be constructed, and is given in the Appendix.

The enlarged Fock space contains also unphysical states which must be eliminated by imposing constraints as in the original formulation by Kotliar and Ruckenstein,¹⁴

$$\begin{aligned} b_{i+}^\dagger b_{i+} + b_{i-}^\dagger b_{i-} + e_i^\dagger e_i &= 1, \\ b_{i+}^\dagger b_{i+} &= f_{i-}^\dagger f_{i-}, \quad b_{i-}^\dagger b_{i-} = f_{i+}^\dagger f_{i+}, \end{aligned} \quad (5.7)$$

and implemented by means of Lagrange multipliers $\{\lambda_i, \mu_{i+}, \mu_{i-}\}$. The first constraint excludes double occupancy, the other two eliminate the unphysical singly occupied states $b_{i+}^\dagger f_{i+}^\dagger |\text{vac}\rangle$ and $b_{i-}^\dagger f_{i-}^\dagger |\text{vac}\rangle$. The electron density and the z -component of the pseudospin can then be described at each site either by slave boson or by pseudofermion operators,

$$n_i \equiv c_{i+}^\dagger c_{i+} + c_{i-}^\dagger c_{i-} = b_{i+}^\dagger b_{i+} + b_{i-}^\dagger b_{i-} = f_{i+}^\dagger f_{i+} + f_{i-}^\dagger f_{i-}, \quad (5.8)$$

$$T_i^z = \frac{1}{2}(b_{i+}^\dagger b_{i+} - b_{i-}^\dagger b_{i-}) = \frac{1}{2}(f_{i-}^\dagger f_{i-} - f_{i+}^\dagger f_{i+}). \quad (5.9)$$

The other two components of the pseudospin operator can only be represented as

$$T_i^+ = b_{i+}^\dagger b_{i-} f_{i-}^\dagger f_{i+}, \quad (5.10)$$

$$T_i^- = b_{i-}^\dagger b_{i+} f_{i+}^\dagger f_{i-}, \quad (5.11)$$

and cannot be reduced to expressions in terms of either slave bosons or pseudofermions alone.⁴²

As in the spin case one further has to renormalize the bosonic factor in Eq. (5.4) in order to recover, when a mean-field approximation is going to be made and the constraints are no longer rigorously obeyed, the correct unrenormalized hopping for the pseudofermions in the uncorrelated ($U=0$) limit. The renormalized boson factors take the form

$$z_{i\pm}^\dagger = \frac{b_{i\pm}^\dagger e_i}{\sqrt{(1 - e_i^\dagger e_i - b_{i\mp}^\dagger b_{i\mp})(1 - b_{i\pm}^\dagger b_{i\pm})}}, \quad (5.12)$$

where it is important that the operator expression under the square root in the denominator is $U(1)$ invariant, so that z_{i+}^\dagger (z_{i-}^\dagger) transforms under Eqs. (5.6) exactly as b_{i+}^\dagger (b_{i-}^\dagger). Then the Hamiltonian in the slave boson representation at $U=0$ becomes

$$\begin{aligned} \mathcal{H}_{U=0} = & -\frac{1}{2}t \sum_{\alpha} \sum_{\langle ij \rangle \parallel \alpha} [z_{i+}^\dagger f_{i-}^\dagger f_{j-} z_{j+} + z_{i-}^\dagger f_{i+}^\dagger f_{j+} z_{j-} \\ & + \gamma (e^{-i\chi_\alpha} z_{i+}^\dagger f_{i+}^\dagger f_{j+} z_{j-} + e^{+i\chi_\alpha} z_{i-}^\dagger f_{i-}^\dagger f_{j-} z_{j+})] \\ & - \sum_i \lambda_i (b_{i+}^\dagger b_{i+} + b_{i-}^\dagger b_{i-} + e_i^\dagger e_i - 1) \\ & - \mu \sum_{i\lambda} f_{i\lambda}^\dagger f_{i\lambda} + \sum_{i\lambda} \mu_{i\lambda} (b_{i\lambda}^\dagger b_{i\lambda} - f_{i\lambda}^\dagger f_{i\lambda}), \end{aligned} \quad (5.13)$$

with $\lambda = \pm$ and $\bar{\lambda} = -\lambda$. The Hamiltonian commutes with the constraints and thus does not connect the physical and the unphysical subspaces of Fock space.

In the mean-field approximation we replace the boson operators by their averages. In order not to spoil the cubic invariance only their amplitudes are replaced by c -numbers, while their phases are prescribed to behave still according to Eqs. (5.6).⁴³ So we set for the boson invariants

$$\begin{aligned} \langle b_{i+}^\dagger b_{i+} \rangle &\equiv \bar{b}_{i+}^2, \\ \langle b_{i-}^\dagger b_{i-} \rangle &\equiv \bar{b}_{i-}^2, \\ \langle e_i^\dagger e_i \rangle &\equiv \bar{e}_i^2, \end{aligned} \quad (5.14)$$

where \bar{b}_{i+} , \bar{b}_{i-} , and \bar{e}_i are real quantities, i.e., they do not contain any nontrivial phase.⁴¹ For the offdiagonal, noninvariant, two-boson products we set

$$\begin{aligned} \langle b_{i+}^\dagger e_i \rangle &\equiv \bar{b}_{i+} \bar{e}_i e^{-i\hat{\vartheta}_i}, \quad \langle e_i^\dagger b_{i+} \rangle \equiv \bar{b}_{i+} \bar{e}_i e^{+i\hat{\vartheta}_i}, \\ \langle b_{i-}^\dagger e_i \rangle &\equiv \bar{b}_{i-} \bar{e}_i e^{+i\hat{\vartheta}_i}, \quad \langle e_i^\dagger b_{i-} \rangle \equiv \bar{b}_{i-} \bar{e}_i e^{-i\hat{\vartheta}_i}, \end{aligned} \quad (5.15)$$

where the phase operator $\hat{\vartheta}_i$ is understood to transform as

$$\hat{U}_i(\theta) \hat{\vartheta}_i \hat{U}_i^\dagger(\theta) = \hat{\vartheta}_i + \theta, \quad (5.16)$$

and in particular assumes the cubic values ϑ_a , ϑ_b , and ϑ_c when the two-boson operator product occurs in an expression taken along the a axis, b axis, or c axis, respectively. The last average of Eqs. (5.14) controls the number of holes in the e_g band, $\bar{e}_i^2 = x$, for a phase with uniform charge density. The constraints give then the following self-consistency conditions,

$$\begin{aligned} \bar{b}_{i+}^2 &= \langle f_{i-}^\dagger f_{i-} \rangle, \quad \bar{b}_{i-}^2 = \langle f_{i+}^\dagger f_{i+} \rangle, \\ \bar{b}_{i+}^2 + \bar{b}_{i-}^2 &= 1 - x, \end{aligned} \quad (5.17)$$

while the renormalization factors become

$$\langle z_{i\pm}^\dagger \rangle \equiv \sqrt{q_{i\pm}} e^{\mp i\hat{\vartheta}_i}, \quad \langle z_{i\pm} \rangle \equiv \sqrt{q_{i\pm}} e^{\pm i\hat{\vartheta}_i}, \quad (5.18)$$

with

$$q_{i\pm} = \frac{x}{1 - \langle f_{i\mp}^\dagger f_{i\mp} \rangle} = \frac{x}{1 - \langle n_{i\pm} \rangle}. \quad (5.19)$$

The exponentials containing $\hat{\vartheta}_i$ can be eliminated from the Hamiltonian by absorbing them in the pseudofermions, according to

$$\hat{f}_{i\pm}^\dagger = e^{\mp i\hat{\sigma}_i} \hat{f}_{i\mp}^\dagger. \quad (5.20)$$

Note that this definition ensures that the $\hat{f}_{i\pm}^\dagger$ transform properly under $U(1)$ in accordance with Eqs. (5.6).

Within the slave boson mean-field approximation one thus finds an effective Hamiltonian for pseudofermions subject to local constraints, and with renormalized hopping. In the case of orbital-ordered phases its precise form depends on the assumed type of state, with the hopping renormalization factors $q_{i\pm}$ either uniform or alternating between two sublattices. Here we present only its simpler form, adequate for uniform phases, such as FO and OL states, in which the renormalization factors and Lagrange parameters can be taken site independent,

$$\begin{aligned} \mathcal{H}_{U=\infty}^{\text{MF}} = & -\frac{1}{2}t \sum_{\alpha} \sum_{\langle ij \rangle \parallel \alpha} [q_+ \hat{f}_{i+}^\dagger \hat{f}_{j+} + q_- \hat{f}_{i-}^\dagger \hat{f}_{j-} + \gamma \sqrt{q_+ q_-} (e^{-i\chi_\alpha} \hat{f}_{i+}^\dagger \hat{f}_{j-} \\ & + e^{i\chi_\alpha} \hat{f}_{i-}^\dagger \hat{f}_{j+})] - \sum_{i\lambda} \mu_\lambda \hat{n}_{i\lambda}, \end{aligned} \quad (5.21)$$

with $\hat{n}_{i\lambda} = \hat{f}_{i\lambda}^\dagger \hat{f}_{i\lambda}$. The present formalism reproduces the results of Kotliar and Ruckenstein for the spin model ($\gamma=0$) with hopping $\frac{1}{2}t$ and gives the same results as the Gutzwiller approximation,⁴⁴ and so q_+ and q_- will be called also Gutzwiller factors.

The ordered states can be obtained within the present KR slave boson approach by a proper choice of the Lagrange multipliers. For instance, the FO+ state is now obtained from Eq. (5.21) by imposing $\langle \hat{n}_{i-} \rangle = 0$ by means of the condition $\mu_- = -\infty$ (while $\mu_+ = 0$). Such states do not experience any band narrowing, as double occupancy is rigorously eliminated at $U=\infty$, and the correlation energy vanishes.⁴⁵ As a result, only the $\varepsilon_{U=\infty}^{\text{FO}}(\mathbf{k}) = -tA_{\mathbf{k}}$ band is partly filled in the FO+ state, while the $\varepsilon_{U=\infty,\pm}^{\text{AO}}(\mathbf{k}) = \pm \gamma t B_{\mathbf{k}}$ bands are filled in the AO± state. Real orbital-ordered states can also be obtained, using the formalism described in the Appendix. Therefore in the $U=\infty$ limit one reproduces the results of the HF approximation described for these states in Sec. IV.

B. Nature of the orbital liquid state

A qualitatively new solution, however, is obtained within the present approximation for the *disordered* state, where double occupancies are on average eliminated by the slave bosons, and this correlation effect leads to an increase of the kinetic energy. The minimum energy is obtained when the pseudofermion densities are equal, $\langle \hat{n}_{i+} \rangle = \langle \hat{n}_{i-} \rangle = \frac{1}{2}(1-x)$, and the Gutzwiller renormalization factors take the simple form,

$$q(x) = q_{\pm}(x) = \frac{2x}{1+x}. \quad (5.22)$$

Then the pseudofermion bands,

$$\begin{aligned} \varepsilon_{U=\infty,\pm}^{\text{OL}}(\mathbf{k}) &= q(x) \varepsilon_{U=0,\pm}(\mathbf{k}) \\ &= -tq(x)[A_{\mathbf{k}} \pm \gamma B_{\mathbf{k}}], \end{aligned} \quad (5.23)$$

represent formally the superposition of the FO+ and AO± bands given by Eq. (3.36), typical for uncorrelated e_g elec-

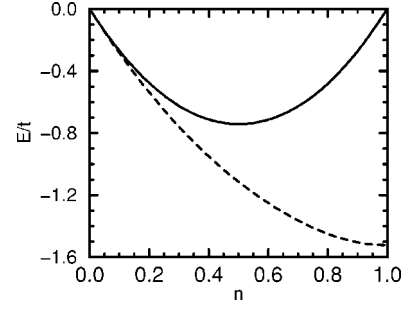


FIG. 5. Kinetic energies E/t of the OL state for uncorrelated ($U=0$, dashed line) and correlated ($U=\infty$, full line) e_g electrons (at $\gamma=1$), as functions of the electron density n .

trons, but now *renormalized by correlations*. They interpolate correctly between the case of uncorrelated electrons in an empty band ($x \approx 1$) and a Mott insulator at half-filling ($x=0$) where the dispersion is fully suppressed, as illustrated in Fig. 5. Owing to the Gutzwiller factors the kinetic energy has a minimum at filling $n=0.5$, and approaches zero at $n=1$. Thus the kinetic energy has a similar doping dependence to that found in a spinless fermion model, i.e., for fermions with a *single* orbital flavor. As in the spin case,⁴⁶ one can argue that at $x \sim 0$ strong correlations lead to an effective exclusion principle between the two degrees of freedom also in \mathbf{k} space, i.e., for each momentum \mathbf{k} only one orbital flavor may be occupied.

This OL state is fully isotropic in the sense that the mean-field values of the pseudospin operators vanish, i.e.,

$$\langle T_i^x \rangle = \langle T_i^y \rangle = \langle T_i^z \rangle = 0. \quad (5.24)$$

For the z -component this follows immediately from Eq. (5.9) once $\bar{b}_{i+}^z = \bar{b}_{i-}^z$. For the other components we apply Eqs. (5.15) and (5.20) to Eq. (5.10) and obtain

$$\langle T_i^+ \rangle = \bar{b}_{i+} \bar{b}_{i-} e^{-2i\hat{\sigma}_i} \langle \hat{f}_{i+}^\dagger \hat{f}_{i+} \rangle = \frac{1}{2}(1-x) \langle \hat{f}_{i+}^\dagger \hat{f}_{i-} \rangle, \quad (5.25)$$

and similarly for $\langle T_i^- \rangle$. The pseudofermion averages can be determined by making use of Fourier transformation: since the Fourier-transformed Hamiltonian (5.21) can be diagonalized analytically, the Fourier-transformed pseudofermion operators can be expressed in terms of the eigenvectors $\{e_{\mathbf{k}+}, e_{\mathbf{k}-}\}$, with the result

$$\begin{aligned} \langle \hat{f}_{\mathbf{k}+}^\dagger \hat{f}_{\mathbf{k}-} \rangle + \langle \hat{f}_{\mathbf{k}-}^\dagger \hat{f}_{\mathbf{k}+} \rangle &= \frac{C_{\mathbf{k}}}{B_{\mathbf{k}}} (\langle e_{\mathbf{k}+}^\dagger e_{\mathbf{k}+} \rangle - \langle e_{\mathbf{k}-}^\dagger e_{\mathbf{k}-} \rangle), \\ \langle \hat{f}_{\mathbf{k}+}^\dagger \hat{f}_{\mathbf{k}-} \rangle - \langle \hat{f}_{\mathbf{k}-}^\dagger \hat{f}_{\mathbf{k}+} \rangle &= i \frac{D_{\mathbf{k}}}{B_{\mathbf{k}}} (\langle e_{\mathbf{k}+}^\dagger e_{\mathbf{k}+} \rangle + \langle e_{\mathbf{k}-}^\dagger e_{\mathbf{k}-} \rangle). \end{aligned} \quad (5.26)$$

Since the eigenvalues $\varepsilon_{U=\infty,\pm}^{\text{OL}}(\mathbf{k})$ are cubic invariant [see Eq. (5.23)] in each of the two bands the three states with the components of \mathbf{k} cyclically permuted are either all occupied or all unoccupied, and thus

$$C_+ = \sum_{\mathbf{k}} \frac{\cos k_\alpha}{B_{\mathbf{k}}} \langle e_{\mathbf{k}+}^\dagger e_{\mathbf{k}+} \rangle \quad (5.27)$$

is independent of α , and similarly for C_- . It then follows from the form of $C_{\mathbf{k}}$ and $D_{\mathbf{k}}$ [see Eqs. (3.9) and (3.10)] that the expressions $\langle \hat{f}_{\mathbf{k}+}^\dagger \hat{f}_{\mathbf{k}+} \rangle$, given by Eqs. (5.26), both give zero when summed over the Brillouin zone, and so

$$\langle \hat{f}_{i+}^\dagger \hat{f}_{i-} \rangle = \langle \hat{f}_{i-}^\dagger \hat{f}_{i+} \rangle = 0, \quad (5.28)$$

and Eq. (5.24) follows.

The absence of a preferred orientation of the pseudospin implies that there is no orbital preferentially occupied. In particular, $\langle T_i^x \rangle = 0$ and $\langle T_i^y \rangle = 0$ imply [see Eq. (2.4)] that

$$\begin{aligned} \langle c_{iz}^\dagger c_{iz} - c_{ix}^\dagger c_{ix} \rangle &= 0, \\ \langle c_{iz}^\dagger c_{ix} + c_{ix}^\dagger c_{iz} \rangle &= 0, \end{aligned} \quad (5.29)$$

from which it follows that the same relations hold for the operators $\{c_{iz}'^\dagger, c_{ix}'^\dagger\}$ obtained after an arbitrary $U(1)$ rotation, as is easily verified explicitly or by observing that T_i^x and T_i^y rotate as an E doublet [compare the Appendix]. Thus, the OL is $SU(2)$ symmetric—random complex or random real orbitals are equivalent, and indeed the *identical* OL state is obtained using real orbitals, as shown in the Appendix. This *correlated disordered* OL state with completely randomly occupied orbitals is apparently different from that proposed by Ishihara, Yamanaka, and Nagaoka,⁴⁷ in which the planar orbitals $\{x^2 - y^2, y^2 - z^2, z^2 - x^2\}$ play a prominent role.

C. Absence of the Nagaoka theorem

Before investigating the stability of the OL state in Sec. V D, let us consider the special case of a single hole in a half-filled system. In the spin case ($\gamma=0$) the celebrated Nagaoka theorem,⁴⁸ one of the very few exact results in the theory of itinerant magnetism, then applies: Nagaoka has shown that the ground state is FM when a single hole/electron is added to a half-filled system, described by the spin Hubbard model at $U=\infty$. A central assumption of this theorem is that the kinetic energy conserves the spin flavor (see, e.g., the proof in Ref. 48), precisely the feature not obeyed by the orbital flavor of e_g electrons. Thus at $\gamma \neq 0$ no exact statement can be made for the orbital Hubbard model (2.9) and, *a priori*, one expects that polarized states are harder to stabilize in this case.

We have investigated the consequences of the $SU(2)$ symmetry breaking, i.e., of the pseudospin nonconservation, by analyzing the exact solution for a plaquette (four-site cluster) filled by three electrons, as a function of γ . In the spin model, at $\gamma=0$, the ground state, with kinetic energy $E_{\square} = -0.25t$ per site, is fourfold degenerate, corresponding to maximum spin $S = \frac{3}{2}$ as required by the Nagaoka theorem. At $\gamma > 0$ it splits into four nondegenerate states: the ground state and three excited states (the lowest of them is shown in Fig. 6). The first excited state in the spin model ($\gamma=0$) is doubly degenerate, and this degeneracy is not removed at $\gamma > 0$, and the two states lower their energy when γ increases towards

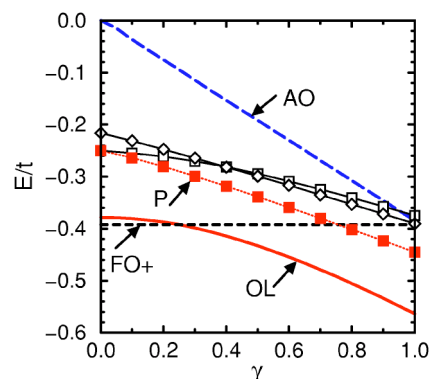


FIG. 6. (Color online) Kinetic energies E per site at electron density $n=0.75$ and $U=\infty$ for increasing off-diagonal hopping $\propto \gamma$ in Eq. (2.9), as obtained in the KR approach for: the OL ground state (solid line), FO+ (dashed line), AO \pm state (AO, long-dashed line), and energy E_{\square} (filled squares) for the ground state of a four-site plaquette (P). Also shown are the energies of the lowest two excited states for the plaquette: a nondegenerate state which splits off the degenerate ground state at $\gamma=0$ (empty squares), and a doubly degenerate state with finite excitation energy at $\gamma=0$ (diamonds).

$\gamma=1$. For $\gamma \geq 0.4$ this degenerate excited state has already a lower energy than any other excited state (the level crossing is shown in Fig. 6). None of these states can be classified by a pseudospin quantum number. In the genuine orbital case ($\gamma=1$) the kinetic energy per site in the ground state, $E_{\square} \approx -0.44t$, is much lower than in the spin case (at $\gamma=0$), showing that a considerable amount of kinetic energy is gained when the orbitals get disordered and full advantage is taken of the pseudospin-nonconserving hopping. This result suggests that a similar tendency towards disorder should be present in the thermodynamic limit.

D. Stability of the orbital liquid phase

Also for the full 3D model it is instructive to consider, at fixed density, the variation with γ of the total energy E of possible ordered and disordered states. We do so in Fig. 6 at the same filling $n=0.75$ as one has in the plaquette filled by three electrons, in order to enable a comparison with the exact results for that finite system. The energy of the polarized FO+ state does not depend on γ [see Eq. (3.31)], while that of the AO \pm state follows from the dispersion given by Eq. (3.32), and decreases linearly with γ . At $\gamma=1$ it comes very close to that of the FO+ state, but remains still a little bit higher. At $\gamma=0$ the polarized FO+ phase has a lower energy than the OL state, which confirms that FM states are stable in a range of filling close to $n=1$ in the 3D Hubbard model.⁴⁹ The energy of the OL phase decreases gradually with increasing γ and becomes lower than that of the FO+ phase (which stays constant) at $\gamma \approx 0.25$. It is remarkable that the energy decrease in the OL phase, when going from $\gamma=0$ to $\gamma=1$, is quite large, and actually of similar magnitude as the exact result in the finite system. Hence one finds that in spite of the renormalization of the hopping by $q(1/4) = 0.4$, the (kinetic) energy in the OL state is substantially lower than in the AO \pm state.

Next we consider the variation of the total energy E of

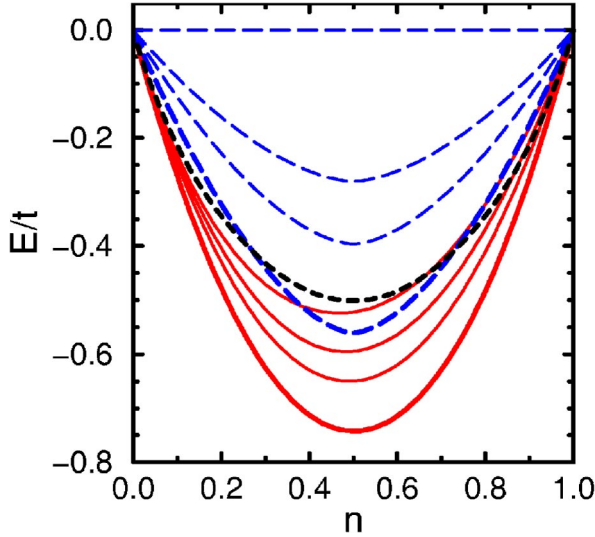


FIG. 7. (Color online) Kinetic energy E in the KR mean-field approximation as functions of n for: AO_{\pm} (long-dashed lines) and OL state (full lines) for increasing $\gamma=0, 0.5, 0.707$, and 1 from top to bottom; the dashed line shows the kinetic energy of the $FO+$ state which is independent of γ .

ordered and disordered *complex* orbital states with electron filling n (Fig. 7). In the spin model ($\gamma=0$) the FM phase has somewhat lower energy than the disordered OL state close to half-filling, in the range $n > 2/3$.⁵⁰ Our approach reproduces in this limit the known result of the slave boson approach, which gives a FM ground state for any bipartite lattice with the density of states being an even function of energy.⁴⁹ When γ is increased, E_{FO+} does not change, whereas $E_{AO_{\pm}}$, initially at zero for $\gamma=0$, decreases $\propto \gamma$, and at $\gamma=1$ surpasses the $FO+$ state at $x=0.27$. Hence the slave boson approach reproduces here the result of the HF approximation for these states.¹⁵ However, in spite of the band narrowing $\propto q(x)$, which is appreciable at these electron densities near half-filling, considerably *more (kinetic) energy is gained in the OL state*. This is basically due to the fact that both hopping channels contribute, which gives rise to the large density of states over the full frequency range, and at small doping in particular [compare Fig. 1(d) with Fig. 2]. We may conclude that the presence of the additional pseudospin-nonconserving hopping channel, associated with the absence of $SU(2)$ symmetry, implies that more kinetic energy can be gained by paying correlation energy than in the spin case, and that this favors the disordered OL state sufficiently to make its energy lower than those of the complex orbital-ordered states at any value of n .

Finally we compare at $U=\infty$ the energies of *all* states, both with complex and real orbitals, varying n and γ . One finds that AO states are never stable in this limit of strong correlation, while FO states are stable only at small γ (Fig. 8). At $\gamma=0$ (the spin case) the $FO+$ and FOx (FOz) states are necessarily degenerate, but at any $\gamma > 0$ the phases with ordered real orbitals have lower energy, with FOz (FOx) being more stable at $n < 0.71$ ($n > 0.71$). The range of FO order shrinks gradually with increasing γ , and above $\gamma \approx 0.94$ the OL phase is stable in the entire range of n . We argue that at finite U the kinetic energy will become even more dominant

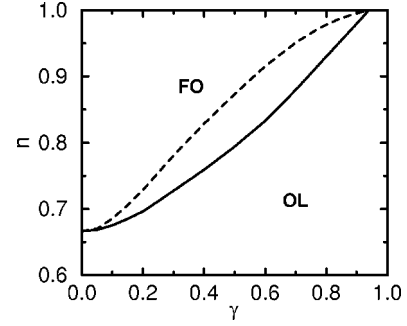


FIG. 8. Region of stability of the FO states at $U=\infty$ as a function of γ , the transition to the OL state from the $FOx(z)$ and complex $FO+$ state are shown by the full and dashed line, respectively.

and thus will strongly favor disorder, except near $n \approx 1$ where SE stabilizes real-orbital AO order.^{2-4,6,24} We thus conclude that for the e_g orbital Hubbard model ($\gamma=1$) doping triggers a crossover to the OL state *at any* U , supporting earlier conjectures that such a disordered state is realized.^{47,51}

E. Brinkman-Rice transition at $n=1$

At half-filling ($n=1$) it is straightforward to apply the finite- U version of the KR formalism,¹⁴ and investigate the generic metal-insulator transition in the orbital disordered phase, ignoring the AO order promoted by the SE. Here one introduces as a counterpart to the bosons e_i which control the empty configurations $|0\rangle = e_i^\dagger |\text{vac}\rangle$, also bosons d_i which control the double occupancies $c_i^\dagger c_{i+1}^\dagger |0\rangle = d_i^\dagger f_{i+1}^\dagger f_{i+1} |\text{vac}\rangle$. The mean-field approximation gives then the renormalization factor (at $n=1$),¹⁴

$$\eta(d) = 8d^2(1 - 2d^2), \quad (5.30)$$

where $d = \langle d_i \rangle$ is the average amplitude of a doubly occupied configuration in the ground state. The bands are then given by the dispersion for free electrons (3.35) renormalized by $\eta(d)$,

$$\varepsilon_{U,\pm}^{\text{OL}}(\mathbf{k}) = \eta(d)\varepsilon_{U=0,\pm}(k) = -\eta(d)t[A_{\mathbf{k}} \pm \gamma B_{\mathbf{k}}]. \quad (5.31)$$

So the kinetic energy is $\eta(d)\bar{\varepsilon}_0(\gamma)$, where $\bar{\varepsilon}_0(\gamma)$ is the kinetic energy of the uncorrelated OL, obtained by integrating the two bands $\varepsilon_{U=0,\pm}(k)$ [Eq. (3.35)] up to half-filling, while the Coulomb repulsion gives an energy Ud^2 per site.

For the spin model ($\gamma=0$) this problem was solved by Brinkman and Rice,⁵² who showed that an “insulating” state (with $d=0$) sets in above $U_c \approx 8t$ (in the present units). It is well understood by now (see Ref. 22) that this mean-field theory does not give an accurate description of the metal-insulator transition (in particular it ignores all charge fluctuations in the insulating phase, where in reality $d \neq 0$).⁵³ By analogy, one expects that also in the present case $d \neq 0$ at any finite U , and in fact this follows from the large- U expansion analyzed for the ordered phases in Secs. IV B and IV C (for a disordered phase a similar analysis could also be made). Nevertheless, the Brinkman-Rice transition from a “metallic” to an “insulating” state at $n=1$ illustrates nicely the competition between kinetic energy and Coulomb repulsion energy,⁵⁴ and so it is worthwhile to consider the general case,

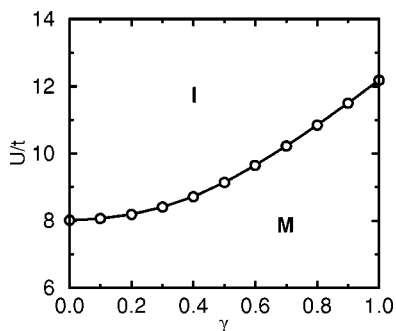


FIG. 9. Metal (M) to insulator (I) transition with increasing U , as obtained in the disordered phase as a function of γ at $n=1$. At $\gamma=1$ (orbital case) the transition occurs in the ground state, while at $\gamma=0$ (spin case) the result of Ref. 52 is reproduced (Ref. 54).

i.e., with arbitrary γ . Then, completely analogously to the spin case, an “insulating” state is found above $U_c(\gamma)=8|\bar{\epsilon}_0(\gamma)|$. Similar to what happens upon doping (i.e., at finite x) in the $U=\infty$ limit considered above, here upon allowing double occupancy (i.e., finite d) at $n=1$, the “metallic” phase gains additional kinetic energy $\propto\gamma$ due to pseudospin-nonconserving hopping which lowers the kinetic energy below the value due to pseudospin-conserving hopping alone (the only one present in the spin case). Therefore the “metallic” phase survives up to a higher value of U than at $\gamma=0$, as shown in Fig. 9.

VI. SUMMARY AND CONCLUSIONS

In this paper we have made a detailed analysis of the e_g -orbital Hubbard model on a cubic lattice, exploring the consequences of the absence of $SU(2)$ symmetry and highlighting them by making a comparison with the familiar $SU(2)$ -symmetric spin Hubbard model. In the first part we studied the orbital-ordered phases, of which there is a great variety, precisely because of the lower symmetry, emphasizing the difference between the complex-orbital states which retain cubic symmetry, and the real-orbital states in which cubic symmetry is broken. Analytical results for the order parameter and the energy of each of these phases in the HF approximation at large U/t were presented, demonstrating that the total energy can be conveniently divided into two contributions: a kinetic energy $\propto t$ given by the $U=\infty$ limit, and a SE contribution $\propto t^2/U$. The SE decides about the relative stability of the various phases at half-filling, while the kinetic energy contributes and finally becomes dominant upon doping. This analytical treatment allowed us: (i) to demonstrate explicitly that SE contributes in both AO and FO states, (ii) to demonstrate that the real-orbital states have their orbitals aligned with the cubic axes, as well as (iii) to elucidate the structure of the HF phase diagram for the ordered phases obtained numerically.^{20,23,24} We emphasize that these properties of e_g orbital degrees of freedom are essentially different from those of t_{2g} ones because the latter satisfy certain symmetries and are thus conserved in the hopping processes.^{5,55}

In the second part we investigated the disordered orbital-liquid state. We have demonstrated that in the strong-

correlation limit ($U\gg t$) indeed orbital (FO or AO) order is not robust for e_g orbitals, and gets replaced by a disordered (OL) phase, if one goes *beyond* the HF approximation and includes electron correlation effects in the disordered phase as well. This leads us to the conclusion that the HF results,^{20,23,24} suggesting that either the FO+ or the AO± state is realized in a broad range of doping, are particularly misleading for the orbital Hubbard model. Here the present findings agree qualitatively with the results of the self-consistent second-order perturbation theory obtained by Kubo and Hirashima.⁵⁶ The situation could be somewhat different in the 2D case, however, where a tendency towards particular orbital orderings with larger amplitude of x^2-y^2 orbitals is favored by geometry.^{28,38}

We considered specifically the $U=\infty$ limit, where the OL competes with fully polarized ordered phases and we have shown that it is more stable than any of either uniform FO [Eq. (4.21)] or staggered AO [Eq. (4.22)] states. However, at finite U and for sufficiently low doping x , real-orbital C -AO order is stabilized by a superposition of the SE and the JT effect. Particularly in the regime of low doping the JT interactions might be stronger than the electronic interactions of double-exchange type, and the induced orbital order dictates then the type of magnetic order.^{35,57} This regime is particularly difficult in realistic models for manganites, as the orbital interactions induced by oxygen distortions,⁶ and the orbital polarization around doped holes,⁵⁸ give additional important contributions and support particular types of orbital order. Furthermore, the overall stability of ordered versus disordered (OL) phases changes when a realistic Hund’s coupling is included.⁵⁹ It has been shown that the FM phase shrinks then to a range of doping $0.2\lesssim x\lesssim 0.5$, the A-type AF phase is stable near $x=0.5$, while the C -AF phase takes over at higher hole doping.

Summarizing, the absence of $SU(2)$ symmetry in the e_g -orbital Hubbard model has severe consequences for the properties of the model itself and for the stability of orbital-ordered states. The Nagaoka theorem does not apply to the model of correlated e_g electrons at $U=\infty$, ordered states are harder to realize than in the spin case, and the Brinkman-Rice transition occurs at a higher value of U . The qualitatively different properties of the ordered phases show up most clearly in the *inverted stability* (with respect to the spin case) of the ordered phases with complex orbitals, with ferro (staggered) orbital order favored at small (large) doping. Most importantly, the exciting suggestion that such complex-orbital ordered states could be stable at finite doping^{20,23,24} has been disproved because of the *inherent tendency of e_g systems towards orbital disorder* due to the enhancement of the kinetic energy when $SU(2)$ symmetry is absent. All these features show that several properties of spin systems which are usually taken for granted, such as: (i) the very fact that a ferromagnetic state is an eigenstate of either an itinerant or the Heisenberg Hamiltonian, and (ii) the absence of superexchange in ferromagnetic states—are in fact the consequences of the $SU(2)$ symmetry of the respective spin models.

ACKNOWLEDGMENTS

We thank P. Horsch, G. Khaliullin, D. I. Khomskii, J. Spałek, P. Wölfle, and particularly K. Rościszewski for in-

sightful discussions. A. M. Oleś would like to acknowledge support by the Polish State Committee of Scientific Research (KBN) under Project No. 1 P03B 068 26.

APPENDIX: SLAVE BOSON REPRESENTATION FOR REAL ORBITALS

The real-orbital version of the transformation of the electron operators to slave boson and pseudofermion operators may be derived by making repeated use of the relation between the real and complex orbitals, as given by Eqs. (2.4). Thus with the real-orbital electron operators given by

$$\begin{aligned} c_{iz}^\dagger &= \frac{1}{\sqrt{2}}(c_{i+}^\dagger + c_{i-}^\dagger), \\ c_{ix}^\dagger &= \frac{i}{\sqrt{2}}(c_{i+}^\dagger - c_{i-}^\dagger), \end{aligned} \quad (\text{A1})$$

we similarly define the real-orbital pseudofermion operators by

$$\begin{aligned} f_{iz}^\dagger &= \frac{1}{\sqrt{2}}(f_{i+}^\dagger + f_{i-}^\dagger), \\ f_{ix}^\dagger &= \frac{i}{\sqrt{2}}(f_{i+}^\dagger - f_{i-}^\dagger), \end{aligned} \quad (\text{A2})$$

while for the slave boson operators we set

$$\begin{aligned} b_{iz}^\dagger &= \frac{1}{\sqrt{2}}(b_{i+}^\dagger + b_{i-}^\dagger), \\ b_{ix}^\dagger &= \frac{-i}{\sqrt{2}}(b_{i+}^\dagger - b_{i-}^\dagger). \end{aligned} \quad (\text{A3})$$

Then the fermions (electrons) transform under $U(1)$ rotations as

$$\begin{aligned} \hat{U}_i(\theta)c_{iz}^\dagger\hat{U}_i^\dagger(\theta) &= \cos(\theta/2)c_{iz}^\dagger - \sin(\theta/2)c_{ix}^\dagger, \\ \hat{U}_i(\theta)c_{ix}^\dagger\hat{U}_i^\dagger(\theta) &= \sin(\theta/2)c_{iz}^\dagger + \cos(\theta/2)c_{ix}^\dagger, \end{aligned} \quad (\text{A4})$$

and similarly for the pseudofermions, while the slave bosons transform as

$$\begin{aligned} \hat{U}_i(\theta)b_{iz}^\dagger\hat{U}_i^\dagger(\theta) &= \cos\theta b_{iz}^\dagger + \sin\theta b_{ix}^\dagger, \\ \hat{U}_i(\theta)b_{ix}^\dagger\hat{U}_i^\dagger(\theta) &= -\sin\theta b_{iz}^\dagger + \cos\theta b_{ix}^\dagger. \end{aligned} \quad (\text{A5})$$

The different sign choice in Eq. (A3) as compared to Eqs. (A1) and (A2) makes the slave bosons rotate in the opposite direction as the (pseudo)fermions. This compensates for the doubled rotation angle in the sense that the transformations are identical for slave bosons and (pseudo)fermions when θ is a cubic angle, and so the pairs $\{c_{iz}^\dagger, c_{ix}^\dagger\}$, $\{f_{iz}^\dagger, f_{ix}^\dagger\}$, and $\{b_{iz}^\dagger, b_{ix}^\dagger\}$ all transform as the θ and ϵ component of a cubic E doublet.

Substituting the complex-orbital slave boson representation (5.4) into Eq. (A1) and applying the transformations inverse to Eqs. (A2) and (A3), one obtains the slave boson representation for the real-orbital fermionic operators $\{c_{iz}^\dagger, c_{ix}^\dagger\}$ analogous to Eq. (5.4). The result is

$$\begin{aligned} c_{iz}^\dagger &= +\frac{1}{\sqrt{2}}(b_{iz}^\dagger f_{iz}^\dagger - b_{ix}^\dagger f_{ix}^\dagger)e_i, \\ c_{ix}^\dagger &= -\frac{1}{\sqrt{2}}(b_{ix}^\dagger f_{iz}^\dagger + b_{iz}^\dagger f_{ix}^\dagger)e_i, \end{aligned} \quad (\text{A6})$$

corresponding to a representation of the local states by

$$\begin{aligned} |i0\rangle &= e_i^\dagger|\text{vac}\rangle, \\ |iz\rangle &= c_{iz}^\dagger|i0\rangle = +\frac{1}{\sqrt{2}}(b_{iz}^\dagger f_{iz}^\dagger - b_{ix}^\dagger f_{ix}^\dagger)|\text{vac}\rangle, \\ |ix\rangle &= c_{ix}^\dagger|i0\rangle = -\frac{1}{\sqrt{2}}(b_{ix}^\dagger f_{iz}^\dagger + b_{iz}^\dagger f_{ix}^\dagger)|\text{vac}\rangle. \end{aligned} \quad (\text{A7})$$

One recognizes that Eqs. (A6) are indeed the proper expressions for the E doublet resulting from the product representation $E \otimes E \otimes A_1$.⁶⁰ The expressions (A6) are actually even $U(1)$ -invariant, i.e., after a rotation in orbital space by an arbitrary angle θ , they also hold between the fermion operators $\{c_{iz}^{\prime\dagger}, c_{ix}^{\prime\dagger}\} = \{\hat{U}_i(\theta)c_{iz}^\dagger\hat{U}_i^\dagger(\theta), \hat{U}_i(\theta)c_{ix}^\dagger\hat{U}_i^\dagger(\theta)\}$, transformed according to Eq. (A4), and the slave boson and pseudofermion operators $\{b_{iz}^{\prime\dagger}, b_{ix}^{\prime\dagger}\}$ and $\{f_{iz}^{\prime\dagger}, f_{ix}^{\prime\dagger}\}$, transformed according to Eqs. (A5) and (A4), respectively. Consequently, since the hopping Hamiltonian (2.3) is invariant under a transformation (A4) of the fermion (electron) operators when θ is one of the cubic angles $0, \pm 4\pi/3$ and is accompanied by the corresponding permutation of the cubic axes, this cubic invariance is retained when the Hamiltonian is expressed in terms of the slave boson and pseudofermion operators by means of Eq. (A6).

The constraints given by Eqs. (5.7) are now replaced by

$$\begin{aligned} b_{iz}^\dagger b_{iz} + b_{ix}^\dagger b_{ix} + e_i^\dagger e_i &= 1, \\ b_{iz}^\dagger b_{iz} + b_{ix}^\dagger b_{ix} &= f_{iz}^\dagger f_{iz} + f_{ix}^\dagger f_{ix}, \\ b_{iz}^\dagger b_{ix} - b_{ix}^\dagger b_{iz} &= f_{iz}^\dagger f_{ix} - f_{ix}^\dagger f_{iz}. \end{aligned} \quad (\text{A8})$$

Again the first constraint excludes double-occupancy, as required in the limit $U=\infty$, while the last constraint is readily verified to eliminate the unphysical singly occupied states,

$$\begin{aligned} |iA_1\rangle &= \frac{1}{\sqrt{2}}(b_{iz}^\dagger f_{iz}^\dagger + b_{ix}^\dagger f_{ix}^\dagger)|\text{vac}\rangle, \\ |iA_2\rangle &= \frac{1}{\sqrt{2}}(b_{ix}^\dagger f_{iz}^\dagger - b_{iz}^\dagger f_{ix}^\dagger)|\text{vac}\rangle. \end{aligned} \quad (\text{A9})$$

When the constraints are obeyed rigorously and the unphysical states strictly projected out, operators connecting the physical and unphysical subspaces necessarily vanish identically. Specifically one finds

$$\begin{aligned} b_{iz}^\dagger b_{iz} - b_{ix}^\dagger b_{ix} &= f_{iz}^\dagger f_{iz} - f_{ix}^\dagger f_{ix} = 0, \\ b_{iz}^\dagger b_{ix} + b_{ix}^\dagger b_{iz} &= f_{iz}^\dagger f_{ix} + f_{ix}^\dagger f_{iz} = 0. \end{aligned} \quad (\text{A10})$$

It is obvious from the above that the earlier attempt made in Ref. 61 to construct a real-orbital slave boson representation by means of $c_{iz}^\dagger = b_{iz}^\dagger f_{iz}^\dagger e_i$ and $c_{ix}^\dagger = b_{ix}^\dagger f_{ix}^\dagger e_i$, followed by renormalization of the slave boson factors by

$$\begin{aligned} z_{iz}^\dagger &= \frac{b_{iz}^\dagger e_i}{\sqrt{(1 - e_i^\dagger e_i - b_{ix}^\dagger b_{ix})(1 - b_{iz}^\dagger b_{iz})}}, \\ z_{ix}^\dagger &= \frac{b_{ix}^\dagger e_i}{\sqrt{(1 - e_i^\dagger e_i - b_{iz}^\dagger b_{iz})(1 - b_{ix}^\dagger b_{ix})}}, \end{aligned} \quad (\text{A11})$$

was misguided because it does not conserve the cubic symmetry and is thus bound to lead to spurious results. However, also the present real-orbital representation, though invariant in itself, leaves us with the problem to construct a proper cubic-invariant renormalization. This is not straightforward because the hopping Hamiltonian, when expressed completely in terms of slave boson and pseudofermion operators referring to “z” and “x,” takes a different appearance for each cubic axis, like in Eq. (2.3). Moreover, the apparently plausible renormalization by means of Eqs. (A11) is not allowed even in combination with the representation (A6), because z_{iz}^\dagger and z_{ix}^\dagger as defined by Eqs. (A11) do not constitute a cubic E doublet as their denominators are not cubic invariants. Having them replace $b_{iz}^\dagger e_i$ and $b_{ix}^\dagger e_i$ in Eqs. (A6) would spoil also the cubic E doublet nature of the thus renormalized c_{iz}^\dagger and c_{ix}^\dagger , and so destroy the cubic symmetry of the Hamiltonian. Equally seriously, it would also cause the Hamiltonian to commute no longer with the constraints.

A renormalization not suffering from the above problems and still in the spirit of the Kotliar-Ruckenstein Ansatz¹⁴ is given by

$$\begin{aligned} z_{iz}^\dagger &= \frac{b_{iz}^\dagger e_i}{\sqrt{(1 - e_i^\dagger e_i - \frac{1}{2}n_i^{(b)}) (1 - \frac{1}{2}n_i^{(b)})}}, \\ z_{ix}^\dagger &= \frac{b_{ix}^\dagger e_i}{\sqrt{(1 - e_i^\dagger e_i - \frac{1}{2}n_i^{(b)}) (1 - \frac{1}{2}n_i^{(b)})}}, \end{aligned} \quad (\text{A12})$$

where $n_i^{(b)} = b_{iz}^\dagger b_{iz} + b_{ix}^\dagger b_{ix}$. The mean-field approximation is now made, as in Sec. V A, by replacing only the amplitudes but not the phases by c -numbers. So, for the off-diagonal two-boson products we set, similarly to what was done in Eqs. (5.15),

$$\begin{aligned} \langle b_{iz}^\dagger e_i \rangle &\equiv \langle e_i^\dagger b_{iz} \rangle \equiv \bar{b}_i \bar{e}_i \cos(\alpha_i - \hat{\vartheta}_i), \\ \langle b_{ix}^\dagger e_i \rangle &\equiv \langle e_i^\dagger b_{ix} \rangle \equiv \bar{b}_i \bar{e}_i \sin(\alpha_i - \hat{\vartheta}_i). \end{aligned} \quad (\text{A13})$$

where \bar{b}_i and \bar{e}_i are again real quantities. For the diagonal two-boson products we set

$$\begin{aligned} \langle b_{iz}^\dagger b_{iz} \rangle &\equiv \langle b_{ix}^\dagger b_{ix} \rangle \equiv \frac{1}{2} \bar{b}_i^2 \\ \langle e_i^\dagger e_i \rangle &\equiv \bar{e}_i^2. \end{aligned} \quad (\text{A14})$$

Actually, the real-orbital boson occupation numbers $n_{iz}^{(b)} = b_{iz}^\dagger b_{iz}$ and $n_{ix}^{(b)} = b_{ix}^\dagger b_{ix}$ are not invariants with respect to $U(1)$ rotations, and so one would prefer to set, in accordance with Eqs. (A13), the corresponding diagonal averages equal to

$$\begin{aligned} \langle b_{iz}^\dagger b_{iz} \rangle &\equiv \bar{b}_i^2 \cos^2(\alpha_i - \hat{\vartheta}_i), \\ \langle b_{ix}^\dagger b_{ix} \rangle &\equiv \bar{b}_i^2 \sin^2(\alpha_i - \hat{\vartheta}_i), \end{aligned} \quad (\text{A15})$$

in order to make them transform in the same way as the occupation numbers, by setting also

$$\langle b_{iz}^\dagger b_{ix} \rangle \equiv \langle b_{ix}^\dagger b_{iz} \rangle \equiv \frac{1}{2} \bar{b}_i^2 \sin(2\alpha_i - 2\hat{\vartheta}_i). \quad (\text{A16})$$

However, the expressions (A15) and (A16) do not satisfy Eqs. (A10), and so it appears to be impossible to assign a nontrivial dependence on the phase operator $\hat{\vartheta}_i$ to $\langle b_{iz}^\dagger b_{iz} \rangle$ and $\langle b_{ix}^\dagger b_{ix} \rangle$ and yet simultaneously respect Eqs. (A10).

The issue is immaterial for carrying out the KR procedure, since in a state with uniform density, i.e., with $\bar{e}_i^2 = x$ for all i , it follows from the constraints (A8) that both for Eqs. (A14) and for Eqs. (A15) the amplitude satisfies $\bar{b}_i^2 = 1 - x$, so that

$$\begin{aligned} \langle z_{iz}^\dagger \rangle &\equiv \langle z_{iz} \rangle \equiv \sqrt{2q(x)} \cos(\alpha_i - \hat{\vartheta}_i), \\ \langle z_{ix}^\dagger \rangle &\equiv \langle z_{ix} \rangle \equiv \sqrt{2q(x)} \sin(\alpha_i - \hat{\vartheta}_i). \end{aligned} \quad (\text{A17})$$

Inserting this into Eqs. (A6) and defining new pseudofermions by

$$\begin{aligned} \hat{f}_{iz}^\dagger &= \cos \alpha_i \hat{f}_{iz}^\dagger + \sin \alpha_i \hat{f}_{ix}^\dagger = \cos(\hat{\vartheta}_i - \alpha_i) f_{iz}^\dagger + \sin(\hat{\vartheta}_i - \alpha_i) f_{ix}^\dagger, \\ \hat{f}_{ix}^\dagger &= -\sin \alpha_i \hat{f}_{iz}^\dagger + \cos \alpha_i \hat{f}_{ix}^\dagger = \sin(\hat{\vartheta}_i - \alpha_i) f_{iz}^\dagger - \cos(\hat{\vartheta}_i - \alpha_i) f_{ix}^\dagger, \end{aligned} \quad (\text{A18})$$

where $\{\hat{f}_{iz}^\dagger, \hat{f}_{ix}^\dagger\}$ are related to $\{\hat{f}_{i+}^\dagger, \hat{f}_{i-}^\dagger\}$ [see Eq. (5.20)] by Eqs. (A2), one finds that the mean-field approximation effectively leads to the replacements

$$c_{iz}^\dagger \equiv \sqrt{q(x)} \hat{f}_{iz}^\dagger, \quad c_{ix}^\dagger \equiv \sqrt{q(x)} \hat{f}_{ix}^\dagger. \quad (\text{A19})$$

The kinetic part of the Hamiltonian is thus simply renormalized by the Gutzwiller factor $q(x)$, exactly the same result as $\langle \rangle$ obtained in the complex-orbital approach. As the Hamiltonian is therefore again cubic, it follows that the resulting real-orbital OL is isotropic [i.e., $\alpha_i = \pi/4$ at all sites, and $\langle b_{iz}^\dagger b_{iz} \rangle = \langle b_{ix}^\dagger b_{ix} \rangle = (1-x)/2$], and identical to the OL obtained in the complex-orbital approach.

- ¹Y. Tokura and N. Nagaosa, *Science* **288**, 462 (2000); S. Maekawa, T. Tohyama, S. E. Barnes, S. Ishihara, W. Koshibae, and G. Khaliullin, *Physics of Transition Metal Oxides* (Springer-Verlag, Berlin, 2004).
- ²K. I. Kugel and D. I. Khomskii, *Usp. Fiz. Nauk* **136**, 621 (1982) [*Sov. Phys. Usp.* **25**, 231 (1982)]; A. M. Oleś, L. F. Feiner, and J. Zaanen, *Phys. Rev. B* **61**, 6257 (2000).
- ³A. M. Oleś, *Phys. Status Solidi B* **236**, 281 (2003).
- ⁴L. F. Feiner, A. M. Oleś, and J. Zaanen, *Phys. Rev. Lett.* **78**, 2799 (1997).
- ⁵G. Khaliullin and S. Maekawa, *Phys. Rev. Lett.* **85**, 3950 (2000); G. Khaliullin, *Phys. Rev. B* **64**, 212405 (2001); G. Khaliullin, P. Horsch, and A. M. Oleś, *Phys. Rev. Lett.* **86**, 3879 (2001).
- ⁶L. F. Feiner and A. M. Oleś, *Phys. Rev. B* **59**, 3295 (1999).
- ⁷M. Imada, A. Fujimori, and Y. Tokura, *Rev. Mod. Phys.* **70**, 1039 (1998); E. Dagotto, T. Hotta, and A. Moreo, *Phys. Rep.* **344**, 1 (2001); E. Dagotto, *Nanoscale Phase Separation and Colossal Magnetoresistance* (Springer-Verlag, Heidelberg, 2003).
- ⁸C. Zener, *Phys. Rev.* **82**, 403 (1951).
- ⁹A. Weiße, J. Loos, and H. Fehske, *Phys. Rev. B* **64**, 054406 (2001); **68**, 024402 (2003).
- ¹⁰R. Maezono, S. Ishihara, and N. Nagaosa, *Phys. Rev. B* **57**, R13993 (1998); **58**, 11583 (1998).
- ¹¹S. E. Barnes, *J. Phys. F: Met. Phys.* **6**, 115 (1976); **6**, 1376 (1976).
- ¹²A. M. Oleś and L. F. Feiner, *Phys. Rev. B* **65**, 052414 (2002).
- ¹³Y. Endoh and K. Hirota, *J. Phys. Soc. Jpn.* **66**, 2264 (1997).
- ¹⁴G. Kotliar and A. E. Ruckenstein, *Phys. Rev. Lett.* **57**, 1362 (1986).
- ¹⁵A. Takahashi and H. Shiba, *Eur. Phys. J. B* **5**, 413 (1998).
- ¹⁶J. van den Brink and D. I. Khomskii, *Phys. Rev. Lett.* **82**, 1016 (1999).
- ¹⁷The seemingly illogical sign choice is in accordance with the Jahn-Teller literature and makes sure that T_i^z [see Eq. (2.5)] and not $-T_i^z$ is the electronic part of the conserved local pseudo angular momentum $J_i = (q_{i\theta}p_{i\epsilon} - q_{i\epsilon}p_{i\theta})/\hbar + T_i^z$ in the Jahn-Teller problem with local Jahn-Teller interaction $\propto q_{i\theta}T_i^x + q_{i\epsilon}T_i^y = \frac{1}{2}[(q_{i\theta} - iq_{i\epsilon})T_i^+ + (q_{i\theta} + iq_{i\epsilon})T_i^-]$, where $q_{i\theta}$ and $q_{i\epsilon}$ are the coordinates of the degenerate vibrational modes at site i , and $p_{i\theta}$ and $p_{i\epsilon}$ are the conjugate momenta; compare: H. C. Longuet-Higgins, U. Öpik, M. H. L. Pryce, and R. A. Sack, *Proc. R. Soc. London, Ser. A* **244**, 1 (1958); R. Englman, *The Jahn-Teller Effect in Molecules and Crystals* (Wiley, London, 1972), Sec. 3.2.1.
- ¹⁸J. Klauder, *Phys. Rev. D* **19**, 2349 (1979).
- ¹⁹Note that θ_i is the azimuthal, not the polar angle. Here we thus follow the common practice in the orbital and Jahn-Teller literature. However, we do not follow the Jahn-Teller convention of replacing $-\theta_i/2$ by θ_i , which would yield conveniently $|i\theta_i\rangle = \cos\theta_i|iz\rangle + \sin\theta_i|ix\rangle$ but would upset the standard form of the pseudospin vector Eq. (2.7).
- ²⁰J. van den Brink and D. I. Khomskii, *Phys. Rev. B* **63**, 140416(R) (2001).
- ²¹The complete argument is actually more subtle because the EQM has an off-diagonal matrix element between $|+\rangle$ and $|-\rangle$. The x, y, z components of \mathbf{T} in the complex-orbital basis correspond to the pseudospin components represented in the conventional real basis by the Pauli matrices σ^z , σ^x , and σ^y , respectively, and so only T^x and T^y appear in the JT coupling, while T^z is the electronic part of the conserved pseudo angular momentum; compare Ref. 17.
- ²²P. Fazekas, *Lecture Notes on Electron Correlation and Magnetism* (World Scientific, Singapore, 1999).
- ²³A. Takahashi and H. Shiba, *J. Phys. Soc. Jpn.* **69**, 3328 (2000).
- ²⁴R. Maezono and N. Nagaosa, *Phys. Rev. B* **62**, 11576 (2000).
- ²⁵S.-Q. Shen, R. Y. Gu, Q.-H. Wang, Z. D. Wang, and X. C. Xie, *Phys. Rev. B* **62**, 5829 (2000).
- ²⁶Note that the mixed constraint (3.4) behaves differently from the similar constraint satisfied by slave bosons alone in Eqs. (5.7), where in mean-field approximation the boson amplitudes depend on the actual electron density [see Eqs. (5.17)]. Here the amplitude of the f_i^\dagger fermions controls the boson amplitudes at finite doping, and the constraint remains observed when Eqs. (3.5) are used.
- ²⁷The dispersion of the e_g bands (Ref. 15) associated with the $\{k_a, k_b\}$ components due to the (a, b) planes is also frequently described using $\gamma_{\mathbf{k}}^\pm = \frac{1}{2}(\cos k_a \pm \cos k_b)$ which gives equivalent expressions to those given in Sec. III.
- ²⁸F. Mack and P. Horsch, *Phys. Rev. Lett.* **82**, 3160 (1999).
- ²⁹R. Maezono and N. Nagaosa, *Phys. Rev. B* **61**, 1825 (2000).
- ³⁰A. Koizumi, S. Miyaki, Y. Kakutani, H. Koizumi, N. Hiraoka, K. Makoshi, N. Sakai, K. Hirota, and Y. Murakami, *Phys. Rev. Lett.* **86**, 5589 (2001).
- ³¹T. G. Perring, G. Aeppli, S. M. Hayden, S. A. Carter, J. P. Remeika, and S.-W. Cheong, *Phys. Rev. Lett.* **77**, 711 (1996).
- ³²J. A. Fernandez-Baca, P. Dai, H. Hwang, C. Kloc, and S.-W. Cheong, *Phys. Rev. Lett.* **80**, 4012 (1998).
- ³³It further follows from Eq. (3.15) that for a general (i.e., not “antiferro”) AO state the dispersion reduces in the spin case ($\gamma = 0$) to $\varepsilon_{\mathbf{k}}^{\text{AO}, \pm}(\mathbf{k}) = \pm t \cos(\Theta_{AB}/2)A_{\mathbf{k}}$ [as shown explicitly for the real case by Eq. (3.19)], which is the well-known single-band double-exchange result with Θ_{AB} being the angle between pseudospins \mathbf{T}_A and \mathbf{T}_B [cf. P.-G. de Gennes, *Phys. Rev.* **118**, 141 (1960)].
- ³⁴The orbital order in the low-temperature phase of the undoped 3D manganite LaMnO_3 is in between $C\text{-AO}_{sa}$ and $C\text{-AO}_{ab}$ [see J. Rodríguez-Carvajal, M. Hennion, F. Moussa, A. H. Moudden, L. Pinsard, and A. Revcolevschi, *Phys. Rev. B* **57**, R3189 (1998)].
- ³⁵A. Weiße and H. Fehske, *New J. Phys.* **6**, 158 (2004).
- ³⁶Formally the situation at zero doping is anomalous. The equation for $\cos\theta_-$ remains valid at $x=0$ and so $\theta_- = \pi/2$, i.e., $\theta_A - \theta_B = \pi$, but θ_+ becomes undetermined, implying that the stable real AO solution is “antiferro” ($\mathbf{T}^A = -\mathbf{T}^B$) but that the common axis of the pseudospin vectors has an arbitrary direction in the “equatorial” plane. This is due to the fact that the angle between the pseudospin vectors is determined by the SE energy (see Secs. IV B and IV C), while the average direction is selected by the kinetic energy, which is zero, though, at $x=0$ and thus ineffective.
- ³⁷In order to obtain the equations which include this deviation one should replace $6-4x$ by $(6-4x)\sin^2\theta_-$ in Eqs. (4.26) and (4.29) and also in Eq. (4.29) replace $\gamma C_{\mathbf{k}}$ by $A_{\mathbf{k}} \cos\theta_- + \gamma C_{\mathbf{k}}$, and then determine $\cos\theta_-$ by minimizing the energy. At small x this yields $\cos\theta_- \simeq -(U/3t)x$, as stated in Sec. IV.
- ³⁸Q. Yuan, T. Yamamoto, and P. Thalmeier, *Phys. Rev. B* **62**, 12696 (2000).
- ³⁹W. von der Linden and D. M. Edwards, *J. Phys.: Condens. Matter* **3**, 4917 (1991).
- ⁴⁰While $\hat{U}_i(\theta)$ was expressed in Eq. (5.1) in terms of the original fermions, here it has to be expressed in terms of the slave bosons

- and pseudofermions: $\hat{U}_i(\theta) = \exp(-i\theta T_i^{z(b)}) \exp(-i\theta T_i^{z(f)})$, where $T_i^{z(b)} = b_{i+}^\dagger b_{i+} - b_{i-}^\dagger b_{i-}$ and $T_i^{z(f)} = \frac{1}{2}(f_{i+}^\dagger f_{i+} - f_{i-}^\dagger f_{i-})$.
- ⁴¹R. Frésard and P. Wölfle, *Int. J. Mod. Phys. B* **6**, 685 (1992); **6**, 3087 (1992).
- ⁴²Therefore the present slave boson representation does not simplify the treatment of the Jahn-Teller effect; compare Ref. 17.
- ⁴³This prescription is handled more naturally in a path integral formulation with the boson field represented in the radial gauge, as in Ref. 41, and the modulus fields replaced by their mean-field value. The redefinition of the pseudofermion operators, Eq. (5.20), is equivalent to the local gauge transformation that eliminates the phase fields.
- ⁴⁴M. C. Gutzwiller, *Phys. Rev.* **137**, A1726 (1965); D. Vollhardt, *Rev. Mod. Phys.* **56**, 99 (1984).
- ⁴⁵Equivalent results are therefore obtained for the orbital ordered states by a single slave fermion approach.
- ⁴⁶J. Spałek and W. Wójcik, *Phys. Rev. B* **37**, 1532 (1988); J. Spałek, *ibid.* **40**, 5180 (1989).
- ⁴⁷The nonvariational slave fermion approximation gives a different band renormalization $\propto x$ [S. Ishihara, M. Yamanaka, and N. Nagaosa, *Phys. Rev. B* **56**, 686 (1997)], and underestimates the stability of the OL phase.
- ⁴⁸Y. Nagaoka, *Phys. Rev.* **147**, 392 (1966).
- ⁴⁹B. Moeller, K. Doll, and R. Frésard, *J. Phys.: Condens. Matter* **5**, 4847 (1993).
- ⁵⁰We note that the value of the critical doping $x \approx 0.33$ is very close indeed to $x \approx 0.32$ found for a single spin-flip in the Gutzwiller wave function for a cubic lattice [B. S. Shastry, H. R. Krishnamurthy, and P. W. Anderson, *Phys. Rev. B* **41**, 2375 (1990)].
- ⁵¹R. Kilian and G. Khaliullin, *Phys. Rev. B* **58**, R11841 (1998).
- ⁵²W. F. Brinkman and T. M. Rice, *Phys. Rev. B* **2**, 4302 (1970).
- ⁵³M. Fleck, M. G. Zacher, A. I. Lichtenstein, W. Hanke, and A. M. Oleś, *Eur. Phys. J. B* **37**, 439 (2004).
- ⁵⁴Note, however, that due to the Fermi surface instability the AF phase, with a gap depending on U , has a lower energy in the entire range of U (see, e.g., Ref. 53).
- ⁵⁵A. B. Harris, T. Yildirim, A. Aharony, O. Entin-Wohlman, and I. Y. Korenblit, *Phys. Rev. Lett.* **91**, 087206 (2003); *Phys. Rev. B* **69**, 035107 (2004).
- ⁵⁶K. Kubo and D. S. Hirashima, *J. Phys. Soc. Jpn.* **71**, 183 (2002).
- ⁵⁷M. Daghofer, A. M. Oleś, and W. von der Linden, *Phys. Rev. B* **70**, 184430 (2004); *Phys. Status Solidi B* **242**, 311 (2005).
- ⁵⁸R. Kilian and G. Khaliullin, *Phys. Rev. B* **60**, 13458 (1999).
- ⁵⁹T. Maitra and A. Taraphder, *Phys. Rev. B* **68**, 174416 (2003).
- ⁶⁰J. S. Griffith, *The Theory of Transition Metal Ions* (Cambridge University Press, Cambridge, England, 1971), p. 396.
- ⁶¹A. M. Oleś and L. F. Feiner, *Acta Phys. Pol. A* **97**, 193 (2000).